Charles University

Faculty of Science

Study program: Evolutionary biology (N-EVOBI)

Bc. Dominika Dbalá

Symmetry of green algal cells and their colonies resulting from adaptive phenotypic plasticity under planktonic life history

Symetrie buněk a buněčných kolonií zelených řas jako projev adaptivní plasticity fenotypu při planktonním způsobu života

Master's thesis

Supervisor: prof. RNDr. Jiří Neustupa, CSc.

Prague, 2024

Author's declaration

I hereby declare that I have written my thesis independently using listed references. I have submitted neither this thesis nor its parts to acquire any other academic degree.

Prohlášení autora

Čestně prohlašuji, že jsem nepředložila práci ani její podstatnou část k získání jiného nebo stejného akademického titulu, že jsem práci zpracovala samostatně, a že jsem uvedla všechny použité informační zdroje a literaturu.

In Prague/V Praze, 8. 8. 2024

Dominika Dbalá

Acknowledgements

In particular, I would like to thank my supervisor Jiří Neustupa for his willing cooperation and enlightening insight. I am aware that working with me was sometimes very challenging, but I believe that despite that we managed to mutually enrich each other intellectually. I would also like to thank my family (and my cats), as they have truly been the most understanding during this challenging time, even though some of them could not be physically around. I would also love to express my gratitude to my best friend Majda, who has been an unwavering support, as she knows best what it is like to write a thesis and need a shoulder to lean on. Last but not least I thank my loyal bars where, with a constant supply of refreshments, I was able to keep up with my thoughts and complete this thesis successfully.

Abstract

The ability of a genotype to produce different phenotypic variations under different environmental conditions is called phenotypic plasticity, which in living organisms can manifest as changes in body symmetry. Geometric symmetry is an ideal but unattainable state in nature. If an organism existed in a world without any biotic and abiotic stressors, perhaps we could expect it to be perfectly symmetric. However, the living world is more complex than that and all organisms are constantly affected by countless environmental stressors. That is why we generally observe organisms more or less asymmetric.

Green algae of the genus *Desmodesmus* are well known for their high degree of phenotypic plasticity. These organisms generally form coenobia, i.e. pseudocolonies of individuals originating from the same parent coenobium. Shape changes of this alga have been studied in the past, but mainly as a difference between unicellular and multicellular stage, or spiny or spineless morphotype. What has not received as much attention is the asymmetry of its coenobia. In my thesis, I described how the asymmetry of *Desmodesmus communis* changed under different conditions that occur during a planktonic life. For this I used the highly developed methods of landmark-based geometric morphometrics. It has been discovered that coenobia living in constitutively mixed and semi-mixed environments arise with an increased level of asymmetry. Coenobia living in stationary environments with increased sinking pressure then exhibited significantly lower rates of asymmetry. This asymmetry was most pronounced in the area of the spines that *Desmodesmus communis* bears on its four corners. Furthermore, my analyses showed the highest asymmetry with regards to the transversal axis. Horisontal and vertical asymmetry didn't result in such high proportions in any of the strains studied. The most determinant source of shape variation was identified as the difference between coenobia within the strain. Differences between segments of asymmetry within a single coenobium were significantly lower. Finally, in *Desmodesmus communis*, small young individuals were found to exhibit significantly higher levels of asymmetry than large and old individuals. A relationship between planktonic life history and phenotypic plasticity in the form of asymmetry was successfully demonstrated. My thesis yielded discoveries that contribute to further understanding of the ecology and complex evolution of these coenobial organisms.

Key words: phenotypic plasticity, asymmetry, *Desmodesmus communis*, geometric morphometrics, landmarks, plankton

Abstrakt

Schopnost genotypu vytvářet různé fenotypové variace při různých podmínkách prostředí se nazývá fenotypová plasticita, která se u živých organismů může projevovat jako změny v symetrii těla. Geometrická symetrie je ideální, ale v přírodě nedosažitelný stav. Pokud by organismus existoval ve světě bez jakýchkoliv biotických a abiotických stresorů, snad bychom mohli očekávat, že pak bude dokonale symetrický. Živý svět je však složitější a na všechny organismy neustále působí nesčetné množství stresových faktorů prostředí. Z tohoto důvodu v přírodě spíše pozorujeme organismy více či méně asymetrické.

Zelené řasy rodu *Desmodesmus* jsou známé svou vysokou fenotypovou plasticitou. Tyto organismy obvykle vytvářejí coenobia, tj. pseudokolonie jedinců pocházejících ze stejného mateřského coenobia. Tvarové změny této řasy byly studovány již v minulosti, ale především jako rozdíl mezi jednobuněčným a mnohobuněčným stádiem, případně morfotypem s ostny a bez ostnů. Čemu však nebyla věnována taková pozornost, je asymetrie jejích coenobií. Ve své diplomové práci jsem popsala, jak se asymetrie řasy *Desmodesmus communis* mění za různých podmínek, které nastávají během planktonního způsobu života. K tomu jsem použila vysoce moderní metody *landmark-based* geometrické morfometriky. Bylo zjištěno, že coenobia žijící v konstitutivně míchaném a polomíchaném prostředí vznikají se zvýšenou mírou asymetrie. Coenobia žijící ve stacionárních prostředích se zvýšeným s*inking pressure* pak vykazovala výrazně nižší míru asymetrie. Tato asymetrie byla nejvýraznější v oblasti ostnů, které *Desmodesmus communis* nese na svých čtyřech rozích. Dále mé analýzy ukázaly nejvyšší asymetrii s ohledem na transverzální osu. Horizontální a vertikální asymetrie nedosahovala tak vysokých podílů u žádného ze studovaných kmenů. Jako nejvýznamnější zdroj tvarové variability byl identifikován rozdíl mezi coenobii v rámci kmene. Rozdíly mezi segmenty asymetrie v rámci jednotlivých coenobií byly výrazně nižší. Závěrem bylo u druhu *Desmodesmus communis* zjištěno, že mladí, malí jedinci vykazují významně vyšší úroveň asymetrie než velcí a staří jedinci. Vztah mezi planktonním způsobem života a fenotypovou plasticitou v podobě asymetrie se podařilo úspěšně prokázat. Moje práce přinesla poznatky, které přispívají k dalšímu pochopení ekologie a složité evoluce těchto coenobiálních organismů.

Klíčová slova: fenotypová plasticita, asymetrie, *Desmodesmus communis*, geometrická morfometrika, landmarky, plankton

Contents

1. Introduction

1.1 Thesis aims

The aim of my thesis is to demonstrate another potential explanation for the diverse phenotypic plasticity of the green algal species *Desmodesmus communis*. Various environmental influences as a source of phenotypic plasticity in the coenobia of this alga have been studied in the past. However, I have chosen to focus on how the conditions prevailing in its natural environment, the plankton, affect its shape.

In my thesis, I plan to observe how coenobia from four genetically isolated strains change their shape through simulations of three possibly occurring planktonic conditions. Mixed, stationary-mixed and stationary condition will be induced as a substitute for the natural environment in constitutively mixed, partially mixed and unmixed water bodies. I suspect that coenobia living in the mixed environment will form highly symmetric coenobia, as the turbulent environment requires the ability to adapt. Conversely, I assume that coenobia living in an unmixed water will arise asymmetrically, as there is no longer a reason to invest energy in staying in the water column, as the sinking pressure is simply too immense. The second aim of my work is be to describe which axis of asymmetry (horisontal, vertical, transversal) is most determinant for the shape of *Desmodesmus communis*. In other words, which asymmetry axis changes the most under different planktonic conditions?

The second part of my thesis is designed to describe the relationship between the size of the coenobium and its asymmetry. I want to find out if large and older individuals will be less symmetric than small and young individuals. I hypothesize that young individuals will not be weighed down by environmental stressors yet and will therefore be highly symmetric. Conversely, I believe that individuals long affected by external influences will gradually become deformed.

The last part of my thesis is meant to describe the symmetric and asymmetric variation of individual strains of *Desmodesmus communis*. This analysis is intended to describe the shape differences within and between strains more precisely. The analysis of symmetric and asymmetric variability has helped to elucidate the developmental and ecological requirements in other algae previously. Thus, in my thesis I hope to deepen the same understanding of phenotypic plasticity and its implications for the life and evolution of *Desmodesmus communis.*

1.2 Phenotypic plasticity

The term phenotype was first used and defined by the Danish botanist, plant physiologist, geneticist and pharmacist Wilhelm Johannsen in 1909. He was therefore the first person to separate the genome of an organism from its external expressions (Johannsen, 1911).

Phenotype refers to all characteristics of an organism with the exception of genes (West-Eberhard, 2008). However, phenotypes are typically still closely linked to genotypical changes, and it is not a given that they function without a mutual interaction. *Sensu stricto*, we look at the genotype as a sequence of nucleotides in DNA, while the phenotype is its extended manifestation (Baverstock, 2021; McKenna *et al.*, 2022). Prior to the recognition of the epigenetic heredity, the DNA sequence was thought to be the sole driver of evolution (Baverstock, 2021). Accepting the idea that not all in development is caused by genes and their evolutionary processes has opened the door to new perspectives on evolutionary biology and helped clarify previously misunderstood organismal behavior (McKenna *et al.*, 2022).

Phenotypic plasticity is the ability of a genotype to generate different phenotypes due to exposure to a range of environmental factors (Gienapp & Merilä, 2017). This process is often seen as a completely separate from genetic processes. In reality, phenotypic plasticity is very often preceded by a change in gene expression (West-Eberhard, 2008). However, such a proposition does not account for epigenetic changes, which also very often give rise to novel phenotypes, without altering the genome (Duncan *et al.*, 2014). Epigenetic shifts involve primarily DNA methylation and histone modifications. Less discussed epigenetic changes are for instance the effect of DNA abundance in the nucleus or chromosome inactivation etc. (Duncan *et al.*, 2014).

1.2.1 Developmental plasticity and phenotypic flexibility

For the purposes of my thesis, it is important to outline other concepts closely related to phenotypic plasticity. Terms often interchangeably used are phenotypic and developmental plasticity. Developmental plasticity involves irreversible phenotypic changes during the sensitive period of ontogeny. A good example is the growth of protective helmets or spines in *Daphnia*. If the egg is exposed to kairomones (hormones produced by predators) during a sensitive period of development, the *Daphnia* grows protective structures which it then carries for life (Riessen & Gilbert, 2018). Phenotypic plasticity is a more general term that also includes changes in other stages of life (Piersma & Drent, 2003). Polyphenism is a subcategory of developmental plasticity, where different alternative phenotypes arise from one genotype in response to certain environmental conditions (Suzuki *et al.*, 2020). A typical example is the caste differentiation in insects (Yang & Pospisilik, 2019). Phenotypic flexibility represents reversible changes in an individual's life depending on, for example, short-term fluctuations in the environment (Garland, 2011). A common example is the reduction in body size in response to a lack of food resources, for example in the sea urchin *Diadema antillarum* or the sea iguana *Amblyrhynchus cristatus* (Piersma & Drent, 2003). Life-cycle staging is the cyclical changes in the phenotype of an organism depending on seasonality and it's considered a subcategory of phenotypic flexibility (Piersma & Drent).

1.3 Geometric morphometrics

In the 1980's an alternative approach to traditional morphometric methods was proposed. Traditional methods looked at morphology through length measurements, angles and ratios. They combined multivariate methods and quantitative morphology but had many unresolved issues in the methodology as well. For example, it was difficult for researchers to agree on which size correction method to use, because each method gave rise to very different analysis results. Traditional morphometrics has also been unable to represent shape as a whole, which is a major obstacle for studying the shape of most living organisms. Geometric morphometrics became an alternative method and ultimately led Rohlf & Marcus in 1993 to call this approach a revolution in morphometrics (Adams *et al.*, 2004; Rohlf & Marcus, 1993).

Geometric morphometrics is a scientific discipline that aims to mathematically describe the shape of living organisms. The modern approaches to morphometrics nowadays are two: outline methods and landmark methods. Outline methods consist of the analysis of open or closed curves, i.e. perimeters with no designated landmarks, but it is a method little used today (Webster & Sheets, 2010). The method that is typically used today is primarily based on the utilization of landmark data (Adams *et al.*, 2004).

Shape analysis by means of landmarks consists in marking out two or three dimensional points (landmarks). These multidimensional points are the same number for each sample studied and are located in the same positions for all individuals (Webster & Sheets, 2010). It is further necessary to remove all information from these data except for the shape itself and that is: scale, orientation and variation in position. Generalized Procrustes Analysis (GPA) is then used to remove this signal. Only then we can get the unbiased raw shape and are thus able to compare the shapes of all studied objects. The next steps include statistical analysis and graphical representation of the results (Adams *et al.*, 2013)

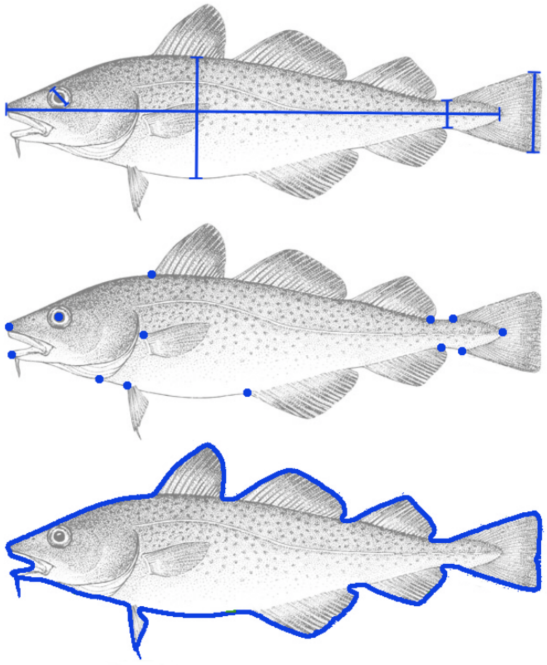

Figure 1. *Visualized differences between morphometric methods.* ***Top****: traditional morphometrics;* ***middle****: landmark-based morphometrics;* ***bottom****: outline-based morphometrics* (Caillon *et al.*, 2018).

Geometric morphometrics is a particularly valuable tool for studying phenotypic plasticity since it can intuitively describe changes in the shape (phenotype) of an organism under different conditions.

1.3.1 Biradial symmetry

The organism I have chosen to study in my thesis is guided by the rules of biradial symmetry. It is a type of symmetry that occurs in many living organisms (algae, plants, ctenophores) (Savriama & Klingenberg, 2011). In summary, it is a hybrid of bilateral and radial symmetry. Bilateral symmetry divides the body of an organism into two equal parts. Organisms with this type of symmetry have only one plane of symmetry that divides the body into a right and a left side. Most butterflies are a very good example, but also, of course, humans. Radial symmetry, on the other hand, divides the body of an organism along many planes of symmetry. An example of radial symmetry may be the sea anemonies (Levin, 2001). Biradial symmetry then divides the body of an organism along two planes of symmetry only (Benítez *et al.*, 2020; Savriama & Klingenberg, 2011). In the study of metazoans, it is the biradial symmetry that is often considered a transitional state between radially and bilaterally symmetric organisms (Martindale & Henry, 1998).

Desmodesmus communis is an organism whose cells can be divided along two perpendicular planes of symmetry (horisontal and vertical) and is therefore an example of biradial symmetry. In my thesis, however, I have chosen a third plane (transversal), which can also be observed.

1.4 Model organism

In my thesis I am focusing on the algal species *Desmodesmus communis*. *Desmodesmus communis* belongs to the order Sphaeropleales and class Chlorophyceae (Guiry & Guiry, 2024).

The class Chlorophyceae is the third most species-rich class of green algae, belonging to the phylum Chlorophyta and the subkingdom Viridiplanteae (Guiry & Guiry, 2024). Most species live in the freshwater environment but a few marine and terrestrial species are also known. Most members of this class are typically known to live in the phytoplankton and phytobenthos of eutrophic waters (Shubert *et al.*, 2014). Species of this class may have a range of thalli types, from coccal to multicellular branching species. The flagellates usually have an apical pair or quartet of equally long flagella (Neustupa, 2015).

Originally, species within the Chlorophyceae were identified primarily by their morphology. However, DNA-based taxonomy later showed that most morphologically determined species are polyphyletic (Neustupa, 2015; Shubert *et al.*, 2014). The class Chlorophyceae is now confidently monophyletic thanks to genetic studies, but uncertainties remain at lower relationship levels (Fučíková *et al.*, 2019). Therefore, the taxonomy of this class is constantly changing and new monophyletic genera are still emerging today.

Currently, the class Chlorophyceae contains the orders Chlamydomonadales, Sphaeropleales, Chaetophorales, Chaetopeltidales and Oedogoniales. The former order Volvocales is now included in

Chlamydomonalades, which includes mainly coccal (*Chlamydomonas*) or colonial flagellates (*Eudorina*, *Volvox*) (Guiry & Guiry, 2024; Krienitz, 2009). All representatives of the order Oedogoniales form filamentous thalli and are typical for their stephanokont zooids - characterized by a ring of flagella around their anterior end (*Bulbochaete*, *Oedogonium*) (Alberghina *et al.*, 2006). Chaetophorales are also typical for their filamentous morphology (*Aphanochaete*, *Chaetophora*) (Guiry & Guiry, 2024; Neustupa, 2015).

Sphaeropleales is a monophyletic but highly heterogeneous group. It consists of both unicellular and coenobial species (Krienitz, 2009). Again these species dominate the plankton of eutrophic waters. Their sexual reproduction is often unknown, so most information is only available on asexual reproduction by zoospores, autospores or aplanospores. The main and most species-rich families within the order Shaeropleales are Scenedesmaceae, Hydrodictyaceae, Selenestraceae, Sphaeropleaceae, Neochloridaceae, Mychonastaceae and Characiaceae (Baudelet *et al.,* 2017).

The genus *Desmodesmus* is one of the most common species in eutrophic plankton in freshwater ponds and rivers. It belongs to the family Scenedesmaceae and is characterized by the formation of coenobia, i.e. pseudocolonies composed of two to sixteen cells always originating from the same generation. The cells of coenobia are often not specialized in any particular way. The marginal cells often bear spines (Shubert *et al.*, 2014). Algae of the Scenedesmaceae family can also be observed as unicellular morphotypes (Trainor, 1998). Sexual reproduction is very rare in this genus and *Desmodesmus* mainly reproduces asexually by autospores or through daughter coenobia formed in the sporangium originating from a vegetative cell (Baudelet *et al.,* 2017).

1.4.1 Phenotypic plasticity of Scenedesmaceae

Most species belonging to the family Scenedesmaceae show extreme levels of phenotypic plasticity and flexibility during their life cycle. In part, this plasticity is manifested as cyclomorphosis, where species produce different ecomorphs depending on seasonality and temperature (Trainor, 1998). This is usually manifested by the formation of unicellular morphs or coenobia depending on environmental conditions. Unicellular morphs are especially common in environments with primarily low cell densities and vice versa (Trainor, 1998). However, phenotypic plasticity in *Desmodesmus* can also arise in the absence of cyclic environmental changes. Well-known examples include the growth of longer spines or the formation of eight to sixteen-celled coenobium in response to grazing pressure or the presence of heavy metals (Baudelet *et al.*, 2017; Lürling, 2003).

Desmodesmus and *Scenedesmus* species have been erroneously described in the past as different species or varieties because of their plasticity and flexibility. However, it was not until 1976 that Frank Trainor questioned the accuracy of these designations. It turned out that they were not always different species, but only different phenotypes of the same genotype (Trainor *et al.*, 1976).

The ability to quickly adapt to changing environmental conditions is probably the reason for the ecological success of the genus *Desmodesmus*. It is also the reason why it was one of the first algae established in laboratory cultures, as it can withstand a really large range of conditions (Lürling, 2003). *Desmodesmus* can cope with changes in environmental conditions, but that doesn't mean they have no effect on its cell development and physiology.

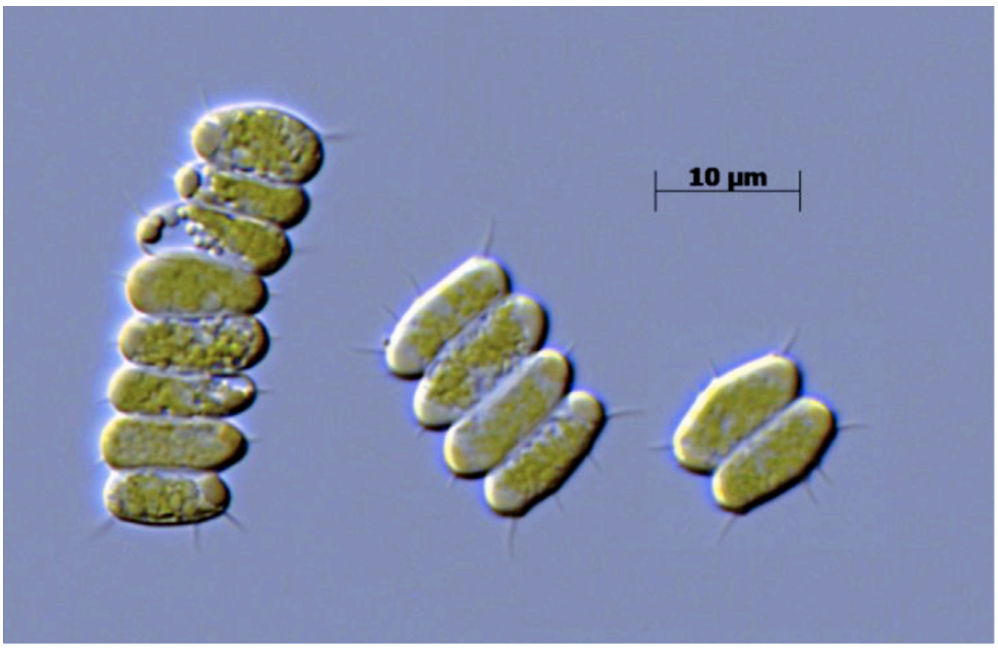

Figure 2. *Difference in the number of cells in the coenobium of Desmodesmus sp. as a result of phenotypic plasticity* (Pozzobon *et al.*, 2020).

In their study, Lürling *et al.*, (2003) focused specifically on the phenotypic plasticity of the genera *Desmodesmus* and *Scenedesmus* in response to the presence of predators. Since these species cannot easily escape predators and their movement is dependent on water currents, it is extremely crucial for them to develop other defenses against grazers. The trigger for this response is the presence of kairomones produced by predators such as *Daphnia* or even smaller rotifers (Kost, 2008). The exposure to kairomones of herbivore grazers in both *Desmodesmus* and *Scenedesmus* has caused the emergence of protective coenobia with larger cell numbers (eight or sixteen). An interesting observation was that protective colonies did not form in the presence of carnivores (Lürling, 2003). However, this was not the only study of its kind. Similar attempts have been made in the past, for example by Hessen & Van Donk (1993). Not only were there large numbers of eight-celled coenobia in the cultures after the addition of *Daphnia*, the coenobia were also heavily armored with spines (Hessen & Van Donk, 1993).

Temperature-dependent phenotypic plasticity has been studied in the genus *Desmodesmus* mainly in the context of seasonality and therefore as a cyclomorphosis. In 1992, Frank Trainor focused his study on the species *Desmodesmus communis*. He observed this species at two different temperatures: 10 and 22 degrees Celsius (Trainor, 1992). It has been demonstrated that the growth rate at 10 degrees Celsius was significantly lower and individuals produced irregular eight or more-celled coenobia with a large number of spines not only at the four usual poles but also at other spots on the cells. Individual cells within the coenobia were significantly larger than the norm and did not match the typical morphology of *Desmodesmus communis*. The terminal and middle cells shared the same morphology and did not develop the typical cell wall between individual cells in the coenobium. A strong resemblance to other species such as *Desmodesmus pannonicus* was observed. Trainor thus drawed attention to the fact that this may reflect phenotypic plasticity rather than genetically distinct *Desmodesmus* species (Trainor, 1992). At 22 degrees Celsius, *Desmodesmus communis* produced morphologically typical coenobia with four or eight cells. The cells were standard in size and the

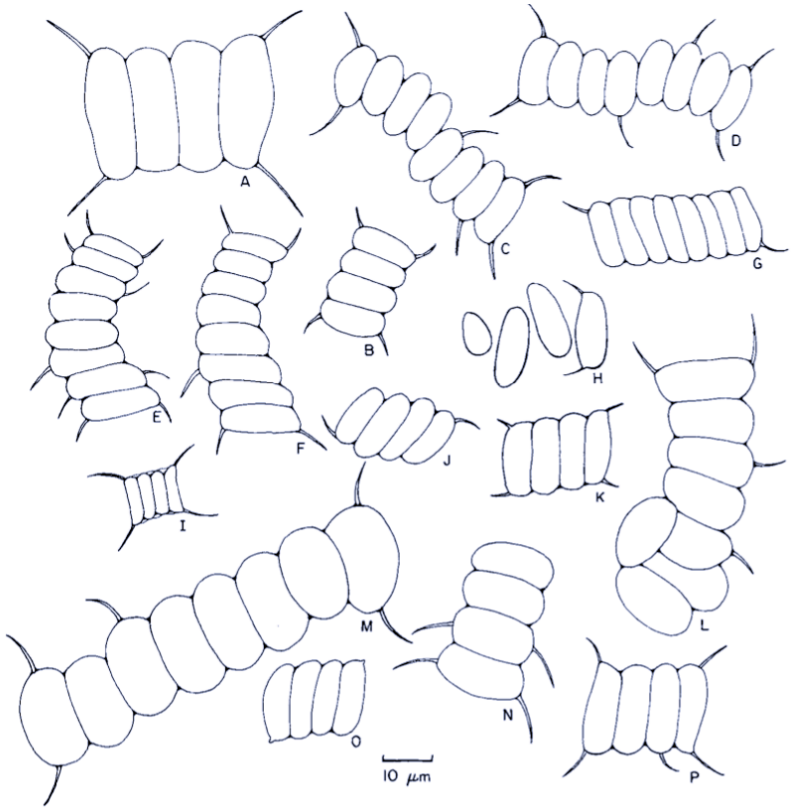

Figure 3. *Different stages in the sequential development of Desmodesmus communis.* ***I.*** *Individual with typical morphology, grown at 22 degrees Celsius;* ***A-H., J-P.*** *Various ecomorphs resulting from growth at temperatures 10 and 22 degrees Celsius* (Trainor, 1992).

spines grew at the typical four poles. Phenotypic changes at 22 degrees Celsius occurred only in older cultures in the form of shorter or no spines. In this study, Trainor points out the importance of paying attention to the sequential development of these organisms. Each growth stage of *Desmodesmus communis* can be classified as a different ecomorph and therefore unfortunately as a different species, as has been erroneously done in the past (Trainor, 1992).

The effect of pH on the phenotypic plasticity of algae has been studied in various species in the past. For example, Černá & Neustupa focused on two acidophilic algal species from the order Desmidiales. *Staurastrum hirsutum* significantly reduced cell size at higher *p*H (around 6.5). *Euastrum binale* var. *gutwinskii*, on the other hand, deepened the notches on its thallus due to higher values of *p*H (Černá & Neustupa, 2009). As mentioned, however, this study focused on acidophilic algae. Algae that naturally grow at higher *p*H are unable to survive low *p*H or produce deformed thalli. This often involves a gradual loss of pigment, shrinking of cells or changes in shape (Gaysina, 2024). Studies of the effect of *p*H on *Desmodesmus* have also been done, but mostly what the implications are for the its growth rate within photobioreactors and therefore its productivity. For example, the study by Bakuei *et al*. found maximum growth rate and biomass of *Desmodesmus* at *p*H value of 8 (Bakuei *et al*., 2014). Yang *et al*. in turn looked at the effect of *p*H on *Scenedesmus obliquus* coenobium formation but again incorporated the aspect of predator presence. In principle, they investigated how kairomone composition and response changes at different *p*H values. This study revealed that induced coenobium formation is the strongest at neutral to slightly alkaline *p*H values, and in acidic water the response to kairomones declines in intensity (Yang *et al*., 2016).

The result of the presence of heavy metals on the phenotypic plasticity of Scenedesmaceae is a better described phenomenon compared to the effect of *p*H. This is attributed to the fact that the Scenedesmaceae family is extremely resistant to pollution, and these studies are therefore generally beneficial for studying the ability of green algae to resist environmental pollution. In 2004, Peña-Castro *et al*. focused on the effect of copper, cadmium and hexavalent chromium on the species *Scenedesmus incrassatulus* (Peña-Castro *et al.*, 2004). In the presence of copper, individuals produced one to two-celled coenobia but did not change cell size at all. Similar behavior was observed in the presence of cadmium, but only after a longer period of time. In the presence of chromium, a very interesting phenomenon was observed. The parent coenobium began to rupture and single cell fragments (autospores) from the original coenobium began to predominate. After some time, however, the ratio of unicellular, two-celled and four-celled coenobia evened out. The size of individual cells was significantly larger. It was observed for all heavy metals that when they were removed from the medium, it resulted in the formation of classic four-celled coenobia after some time (Peña-Castro *et al.*, 2004).

As mentioned above, in my thesis I investigate the effect of water turbulence on the phenotypic plasticity of *Desmodesmus communis*. Water current intensity or turbulence as a natural aspect of planktonic life has been studied in various algal species. A comprehensive experimental study conducted by Padisák *et al.*, (2003) focused on how different algal phenotypes influence sinking rates in the water column. Over thirty species and morphologies of different algae from different kingdoms were included in this study. Algae models were created using PVC-based modeling material and subsequently dropped through a glycerin-filled tube aquarium. For algae at least partially similar in shape to *Desmodesmus communis*, such as *Tetrastrum* (forms a four-celled coenobium with spines), it was observed that the more symmetric the organism, the more it was able to resist sinking pressure and was more likely to persist in the water column (Padisák *et al*., 2003). However, neither *Desmodesmus* nor the algae closest to it in shape were included in this study. In another study, both *Desmodesmus* and *Scenedesmus*, coenobia have been shown to have larger sinking rates than single cell individuals (Lürling, 2003). There may be a simple explanation, namely that coenobia are significantly heavier than unicellular individuals. However, another interpretation could be that

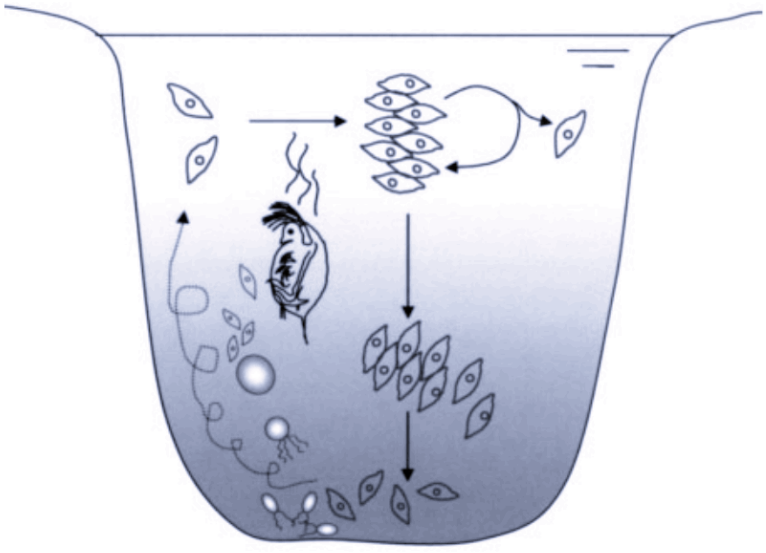

Figure 4. *Possible seasonal life cycle of Scenedesmus sp.* (Lürling, 2003).

coenobia have a greater tendency to be asymmetric. The single cell individuals have greater integration, as the ability to keep one cell symmetric is easier than communicating between multiple cells to maintain colony shape. This is also why the sinking rates of *Scenedesmus* and *Desmodesmus* species have been shown to be much higher in the presence of zooplankton, as they form larger coenobia and sink faster through the water column (Lürling, 2003). Lürling & Van Donk describe this as the price coenobia must pay for resisting predators (Lürling & Van Donk, 2000). In fact, sunken coenobia lose their valuable place in the euphotic zone. However, according to Dehning & Tiltzer, this is not necessarily a disadvantage. In fact, they found that species such as *Scenedesmus acuminatus* can survive up to 10 days in total darkness without rapidly changing its cell counts or growth rate. Thereby, it can be said that the multicellular phenotype is still more profitable for these species, as it represents a very successful escape strategy but does not significantly reduce fitness (Dehning & Tiltzer, 1989). Multicellular coenobia safely divide after sinking and the individual cells then re-enter higher photic zones. Thus, the sinking in the water column provides the individual with escape as well as the time space for subsequent formation of single cell stages that serve as the initial state for the next bloom in the euphotic zone (see Fig. 4.) (Lürling, 2003).

We can see that studies that address phenotypic plasticity in *Desmodesmus communis* do exist. However, these studies are mainly concerned with the number of cells in the coenobium and not quite its symmetry. In the past, the phenomenon of unicellularity in coenobial species as a manifestation of phenotypic plasticity has received particular attention (Morales & Trainor, 2022). Even earlier, this phenomenon was considered as a manifestation of cultivation in culture and as something that hardly occurs in nature. Today it is known that it is often a manifestation of natural seasonality and that, for example, younger populations are composed of more unicellular stages than older populations (Trainor, 1998). But we also know that it is an inevitable step in the ascent back up in the water column after the formation of multicellular coenobia as protection and escape from predators. The study by Padisák *et al.* focused on symmetry, but did not include *Desmodesmus communis*. Similarly, there are studies done on algal symmetry as a geometric phenomenon, but they do not go on to describe what implications symmetry has on algal life history (Savriama & Klingenberg, 2011). In my thesis, I attempt to bridge these two perspectives and look at the effect of symmetry of coenobia on their life history.

2. Material and methods

2.1 Studied strains and their localities

In my thesis I worked with four genetically distinct strains of *Desmodesmus communis*. All samples were taken from locations remote from each other to avoid the potential for clonal strains. The first strain analyzed, CAUP H522 was taken from a collection of Charles University in Prague. However, the strain was originally isolated in 1956 in Greifswald. The other three strains were collected and isolated from a river, a pond and a lake in the Czech Republic.

Strains of *Desmodemus communis* studied	Sampling location	Coordinates	Type of location
Strain A (CAUP H522)	Greifswald, Germany	54.09136842211694, 13.370679967432656	Culture collection
Strain B	Vltava, Prague, Czech Republic	50.06746279641238, 14.414596351786978	River littoral
Strain C	Silvestr, Kostelec nad Vltavou, Czech Republic	49.49604818097088, 14.23509561967346	Pond littoral
Strain D	Krušnohorské oko, Hora Svatého Šebestiána, Czech Republic	50.50395557246769, 13.248469578282336	Lake littoral

Table 1. *List of studied strains and their sampling locations.*

The Vltava River sampling site is located in the very centre of the city. *Desmodesmus communis* was an extremely abundant species in this location. Silvestr Pond is a highly eutrophicated water reservoir. It is located close to a small town and is surrounded by fields and cow pastures. It is also a fish breeding pond, which even at the time of the sampling, contained large quantities of fish feed. The last sampling site, the small lake Krušnohorské Oko, is a semi-artificial shallow lake, partly formed by the backfilling of a mining shaft and partly formed by seeping groundwater. A wind farm is also located in the area.

2.1.1 Sampling methodology

All sampling was conducted during the summer and early fall of 2022 and 2023. Samples were collected using a plankton net. The sampled plankton was then transferred into sampling vials.

2.2 Cell isolation and cultivation

After collection, the samples were microscoped. Using the single-cell selection method, a single coenobium was always cleared of contamination by gradual transfer between slides with clean medium and finally placed in its own growth chamber containing the BBM medium (Andersen, 2004).

Substance	Concentration	Amount added to one litre of medium
KH_2PO_4	8.75 g/500 mL	10 mL
$CaCl_2 \cdot 2H_2O$	12.5 g/500 mL	1 mL
$MgSO_4 \cdot 7H_2O$	37.5 g/500 mL	1 mL
$NaNO_3$	125 g/500 mL	1 mL
K_2HPO_4	37.5 g/500 mL	1 mL
NaCl	12.5 g/500 mL	1 mL
$Na_2EDTA \cdot 2H_2O$	10 g/L	1 mL
KOH	6.2 g/L	
$FeSO_4 \cdot 7H_2O$	4.98 g/L	1 mL
H_2SO_4 (concentrated)	1 mL/L	
H_3BO_3	5.75 g/500 mL	0.7 mL
Trace metal solution*	5,4 mL/L	1mL

Table 2. *BBM medium components* (Stein-Taylor, 1973).

The substances used to prepare the medium can be found in Table 2. In addition, 1 mL of vitamin mixture was added to the final medium.

One individual of *Desmodesmus communis* was always selected for each growth chamber to serve as the base and mother coenobium for the whole strain. In this manner, I obtained cultures that contained genetically identical individuals. The observed changes were thereby most certainly the result of phenotypic plasticity, not genetic polymorphism.

The established single-cell cultures were then left to grow for three weeks to one month at a room temperature. The cultures were microscoped a second time to confirm that they were indeed containing a monoculture of *Desmodesmus communis.* Once the coenobia had multiplied sufficiently, the mixing experiments were carried out.

2.3 Mixing experiments

The aim of the experiments was to simulate the different conditions that life in plankton entails. Therefore, I chose three different conditions that can occur in the water column and from these I derived the treatments themselves. I separated each of the four strains into three separate cultures and subjected them to three different treatments.

The first treatment was the unmixed i.e., the stationary treatment. This treatment consisted of leaving the stationary culture at rest without any kind of turbulence for fourteen days at a room temperature, alternating day and night phases after 12 hours. This treatment was designed to simulate the conditions of an unmixed water body under certain seasonal conditions. For example, this may represent a pond that is not stirred during the summer months. However, it may also, in principle, show different conditions in standing waters and rivers where water is mixed more or less all year round.

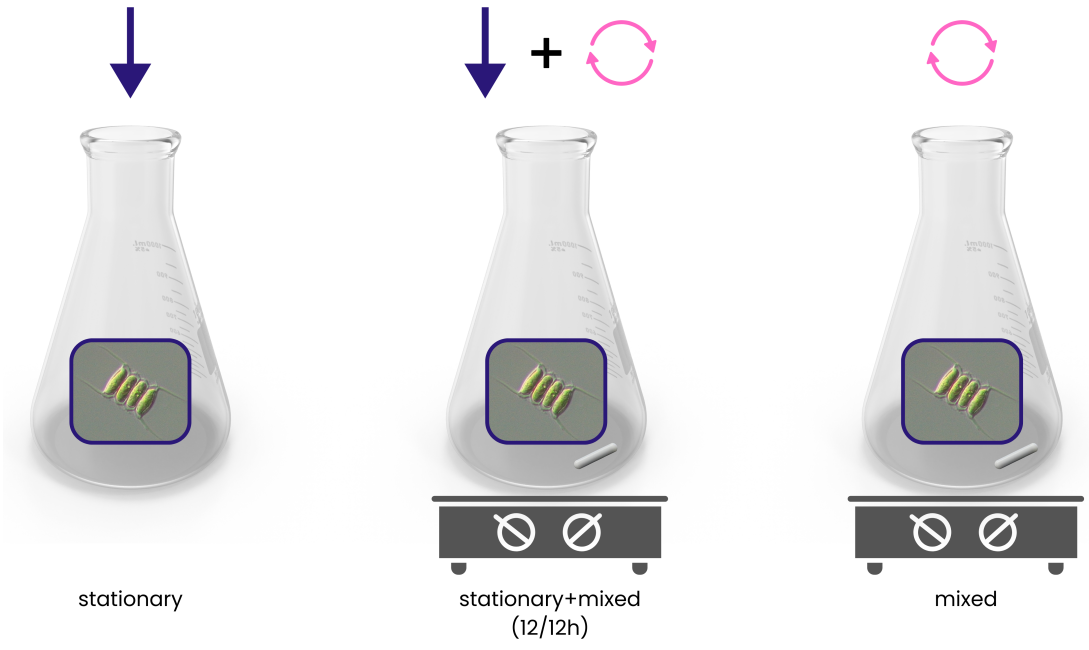

Figure 5. *Visual representation of individual treatments.*

The second treatment i.e., the mixed treatment consisted of placing a magnetic stirrer in the culture and then mixing it on a magnetic pad. This culture was stirred continuously for fourteen days. Day and night phases were alternated in 12 hour intervals. This treatment, in turn, was intended to simulate conditions in a constantly stirred body of water such as a river. Or some ponds and lakes that are stirred continuously or at least very frequently during certain seasons.

The third treatment was the stationary-mixed treatment. In this experiment, the the culture was subjected to mixing for twelve hours and then left at rest for 12 hours without disturbance. The culture changed phases in this manner for fourteen days. Day and night phases were also alternated in 12 hour intervals. The third treatment was intended to represent possible conditions in water bodies where water is stirred and then unstirred for shorter periods of time. This could be, for example, ponds that mix only at night.

Finally, at the end of each experiment, all differently treated cultures from each of the four strains were fixed in 10% ethanol solution to preserve the exact morphologies of the coenobia formed at the time of the experiment end.

2.4 Microphotography

The variously treated cultures were then microscoped at 400x magnification and photographs were obtained with the use of the DM 2000 LED microscope, Leica ICC50 W camera and the LAS X 5.2.1 software. I took photographs of 40 randomly chosen individuals (coenobia) from each treatment from each of the four strains. I only photographed the four-celled coenobia so that I could compare them with each other later in the analysis.

In the end, I acquired 120 photographs representing 120 unique shapes and in total, I worked with 480 distinctive coenobia. I then used the GIMP program (version 2.10.38) to prepare (rotate and crop) each photo so that the photos of the individuals were as similar to each other as possible.

2.5 Geometric morphometrics

As outlined above, I decided to use the properties of landmark-based morphometrics for my analyses. I chose this method because of the modern and highly developed tools provided for its purpose.

2.5.1 Landmark data and processing

Using the versatile geometric-morphometric program tpsUtil (version 1.83) I created an empty TPS file in tpsUtil and then imported the landmark coordinate data into the file during digitization (Rohlf, 2015). I selected the tpsDig2 program (version 2.32) as the tool for inserting landmarks into my data (Rohlf, 2015).

I placed 18 landmarks around each coenobium (see Fig. 6.). Landmarks were chosen to be placed in this way since these marginal locations have the greatest influence on the overall shape of the coenobium and they can be delimited at each of the studied coenobia.

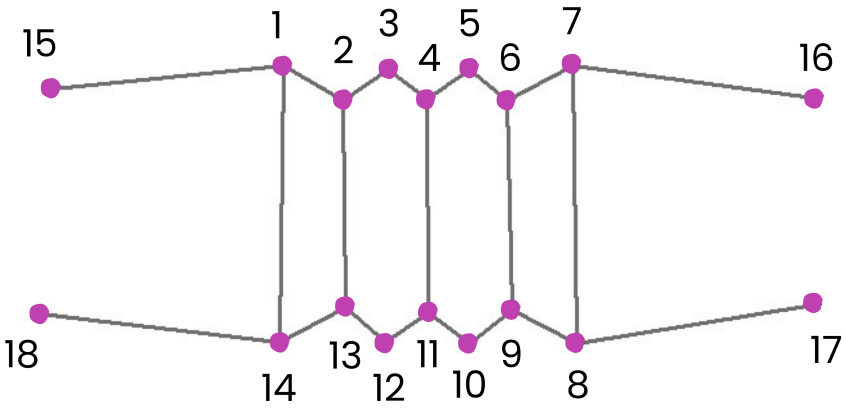

Figure 6. *Distribution of individual landmarks on the coenobium.*

2.6 Analysis No. 1: The difference in asymmetry between treatments and strains

The first analysis was designed to compare the level of horisontal, vertical and transversal axis asymmetry within and between strains and within and between treatments.

The analysis and quantification of biradial symmetry was performed using a utility script in R (R Core Team, 2024). This analysis consisted of a quadruple transformation of the object about its axis. Hence, the analysis worked with four transformed images of the same object and these were: identity, reflection about the vertical axis, a rotation by 180° and a combination of reflection with rotation by 180°. The final combination of the four transformed images produced a consensus that is ideally symmetric in its nature (Savriama *et al.*, 2010). The analysis began by symmetrizing the landmarks and transforming them using Procrustes fit (relabelling and superimposition), which removed the scaling, orientation, and position variation signals from the data (Savriama *et al.*, 2010).

The results of this analysis showed us the overall relative (% PCA of each cell quadrupled) and absolute (standard deviation of scores of object on each axis) values of each type of asymmetry (Savriama *et al.*, 2010). Using Past4 (version 4.15), I then created a graphical visualization of the results and obtained the confidence intervals for the values yielded by each data set (Hammer *et al.*, 2001). Confidence intervals are the range of values we expect to contain our results if we repeat the test. It is a test that tells us how plausible our estimate is and is generated by bootstrap randomization of the original data, respectively their means and medians. The mean can be distorted by outliers, while the median removes this signal and is thus slightly more robust (Hazra, 2017). Confidence intervals for all results of a given treatment and the axis of asymmetry were then compared with each other. The higher the value of the confidence interval, the higher the asymmetry it indicated. Non-overlapping confidence intervals indicated that the studied datasets were indeed significantly different in the degree of asymmetry.

The second part of this analysis was to repeat the identical procedure, but this time I removed the landmarks that marked spines (i.e.: 15, 16, 17, 18) from the data set. This step was taken to gain a deeper understanding from which region of the coenobium the signal with the highest degree of

asymmetry originated from. I suspected from the beginning that the spines would have the greatest influence on the changes in the shape of *Desmodesmus communis*.

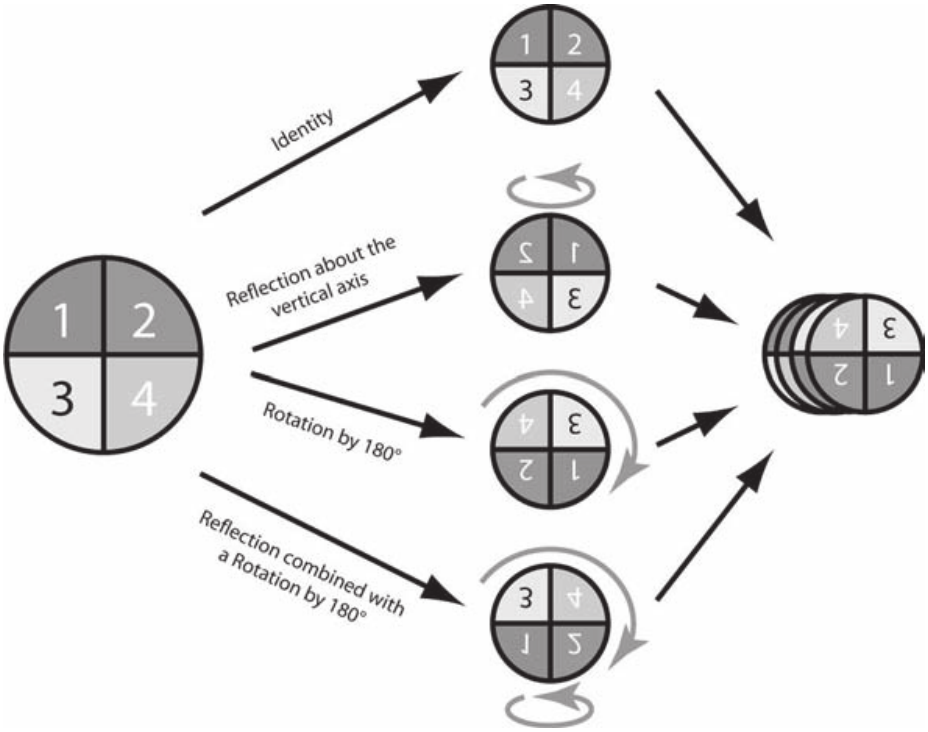

Figure 7. *Visual representation of the analysis and quantification of biradial symmetry* (Savriama *et al.*, 2010).

2.7 Analysis No. 2: The relationship between the size of the coenobium and its asymmetry

In the second analysis I wanted to find out what the relationship is between the size of the coenobium and its asymmetry. In this case, I calculated the centroid size for each coenobium using the tpsRelw program (version 1.17). Centroid size is the square root of the sum of squared distances of a set of landmarks from their centroid (Rohlf, 2015). I chose this procedure to obtain the size of each studied individual. In the Past4 program I then correlated the centroid size data with the corresponding asymmetry data that I obtained in analysis No.1, through multivariate regression.

The resulting slope a values, confidence intervals, Pearson's r values and permutation p values were summarized for later analysis. The slope a is a line intersecting the average of all measured data and therefore represents a linear model of the relationship. The significance of the correlation analysis was then measured using Pearson's r (Nettleton, 2014). The permutation p values arises from the permutation test, which again describes the significance of the result. This test recalculates a particular statistics several times, and if the results are significant, this recalculation should not affect them (Phipson & Smyth, 2010).

Negative Pearson's p value indicated a negative correlation between two variables (Nettleton, 2014). This implies that the lower the Pearson's p value, the more asymmetric the objects were. For my data, this signified that the smaller the coenobia, the more asymmetric the were.

I then visualized the results in morphospace. I observed how the relationship between the size of an individual and the degree of its asymmetry changed. I specifically observed individuals of minimum, average and maximum size. This made it possible to see which size represented the greatest degree of asymmetry.

2.8 Analysis No. 3: Analysis of symmetric and asymmetric variability within the morphospaces of individual strains

The third analysis was designed to provide a broader understanding of the origin of *Desmodesmus communis* asymmetry. PCA analysis was performed to further describe differences in symmetric and asymmetric variation between and within coenobia. In this section, I no longer paid attention to the effect of the treatments themselves, so I removed this signal from the dataset and analyzed the whole strain as a single unit. Using a utility R script, a symmetrized file was then created for each strain - that is, a file of 120 objects (originally 480, since each coenobium was transformed four times). Each object here represented the symmetrized configuration of each coenobium. The next step of the script was to create a quadruple file of 480 objects again. Relative Warps Analysis (RWA), the equivalent of PCA for geometric morphometric data, was performed on these data in tpsRelw program (version 1.17), producing those axes that accurately showed symmetry plus asymmetry components of the variability (Rohlf, 1993). These data were further visualized in morphospace.

3. Results

3.1 Analysis No. 1: The difference in asymmetry between treatments and strains

The goal of analysis No. 1 was to characterize the extent of three different coenobial asymmetry types (axes) in response to three distinct treatments (that emulated various environmental conditions). Next, the collected data for all types of asymmetry and treatment were compared with one another.

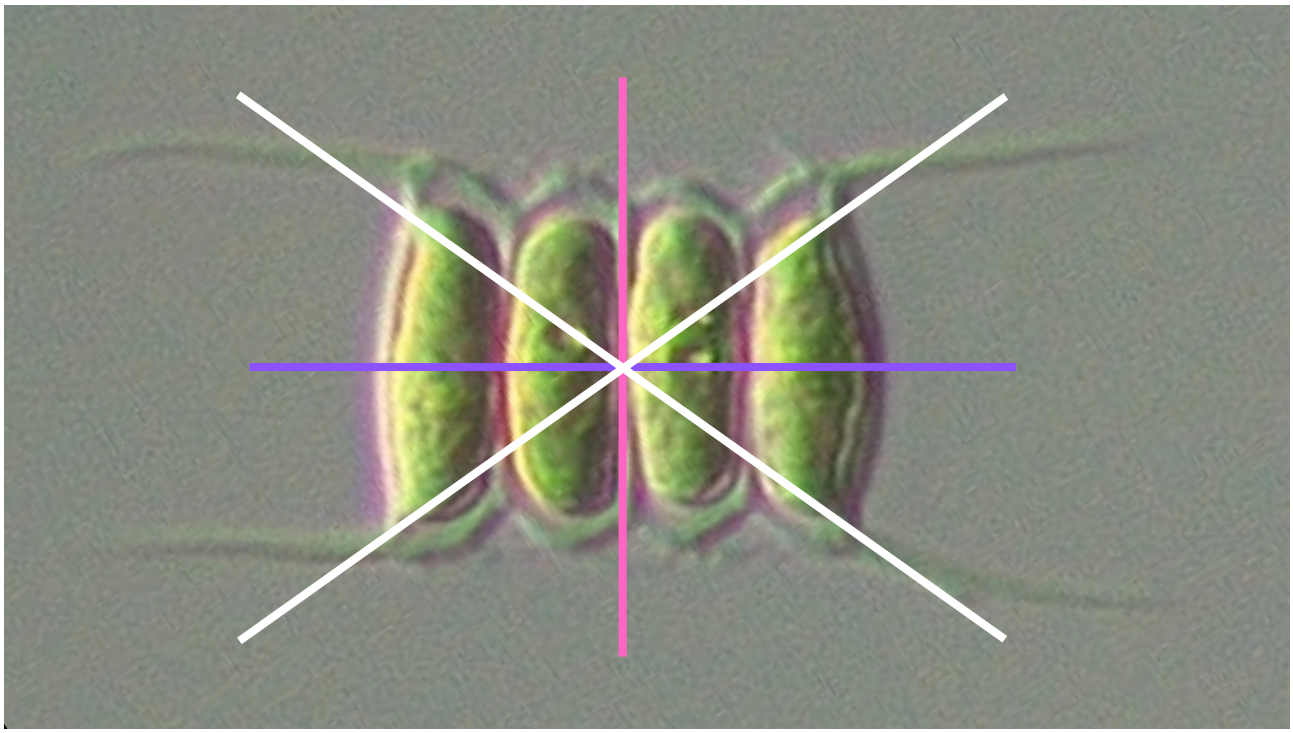

Figure 8. *Distribution of symmetry axes on the coenobium of Desmodesmus communis.*

3.1.1 Analysis with spines

Eighteen landmarks, spread across the coenobium's spines (4) and core (14) were included in the initial section of the analysis

The collection strain CAUP H522 (Strain A) was the first strain to be examined (see Fig. 9.). Table 3., which includes the means, medians, and confidence intervals for each value, documents the significance of the results. In terms of the axes of asymmetry, it was discovered that, for this strain, the vertical axis had the highest degree of asymmetry while still being extremely similar to the horisontal axis. The lowest degree of asymmetry was observed with regards to the transversal axis. This is also

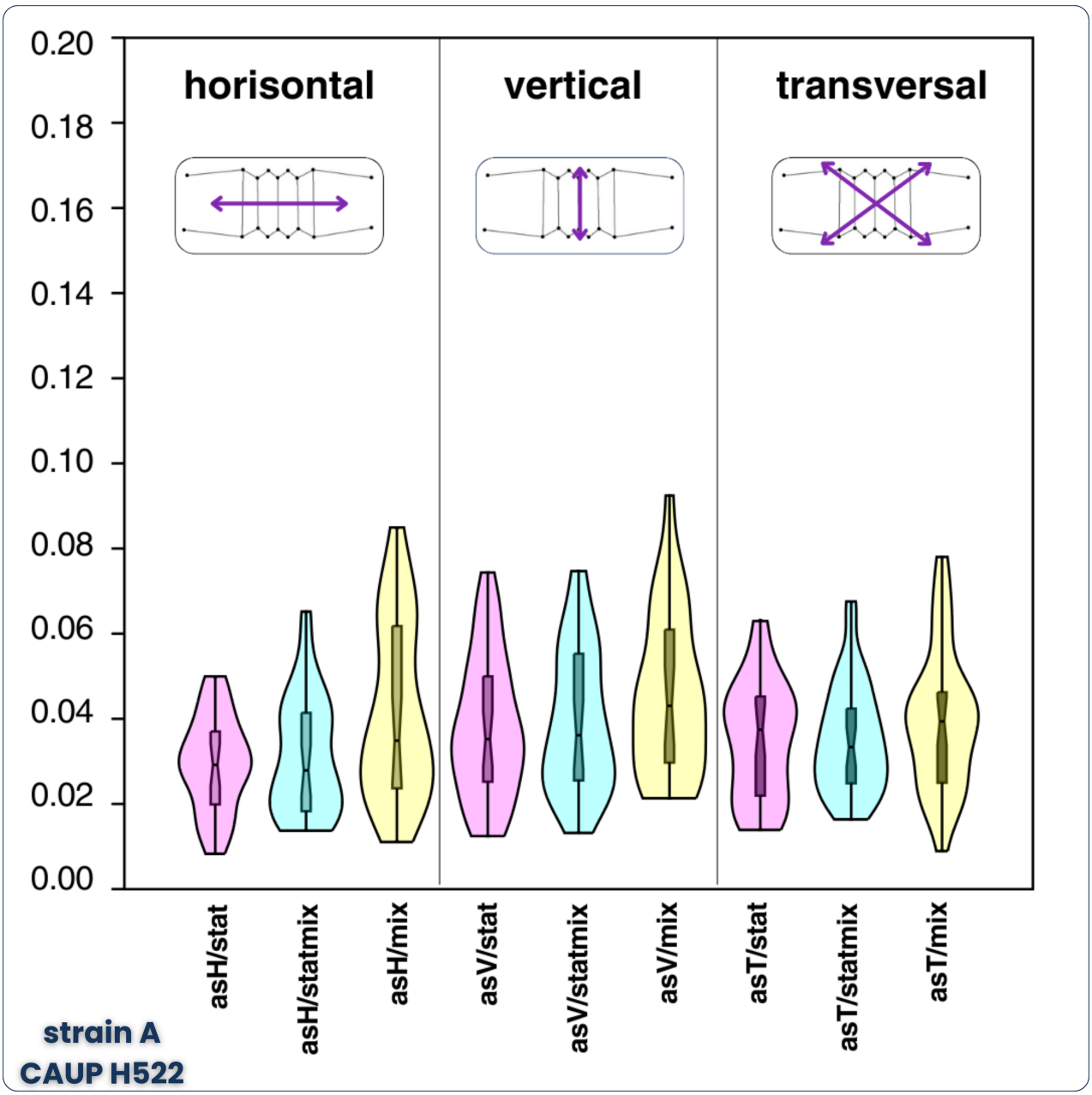

Figure 9. *Graph describing the relationship between treatments and their effect on different types of asymmetry in strain A (spines included). asH = horisontal asymmetry, asV = vertical asymmetry, asT = transversal asymmetry. Stat = stationary treatment, statmix = stationary-mixed treatment, mix = mixed treatment.*

evident in the vertical and horisontal axis mean, median, and confidence intervals, which typically achieved higher values than the transversal axis did.

The mixed treatment was the one that seemed to have the biggest impact on the coenobial asymmetry. The confidence intervals in which the mean and median varied reached higher values and were broader than those of the stationary-mixed and stationary treatment. The transversal axis was the lone exception, reaching its maximum mean under the stationary treatment. The median value, however, was also the highest in the mixed treatment. A similar degree of asymmetry was then expressed by the stationary and stationary-mixed treatment, as can be seen in their confidence intervals for all axes.

Compared to the other strains, in strain A the asymmetry generally did not reach such high values and the intervals in which the asymmetry data varied were significantly lower and narrower.

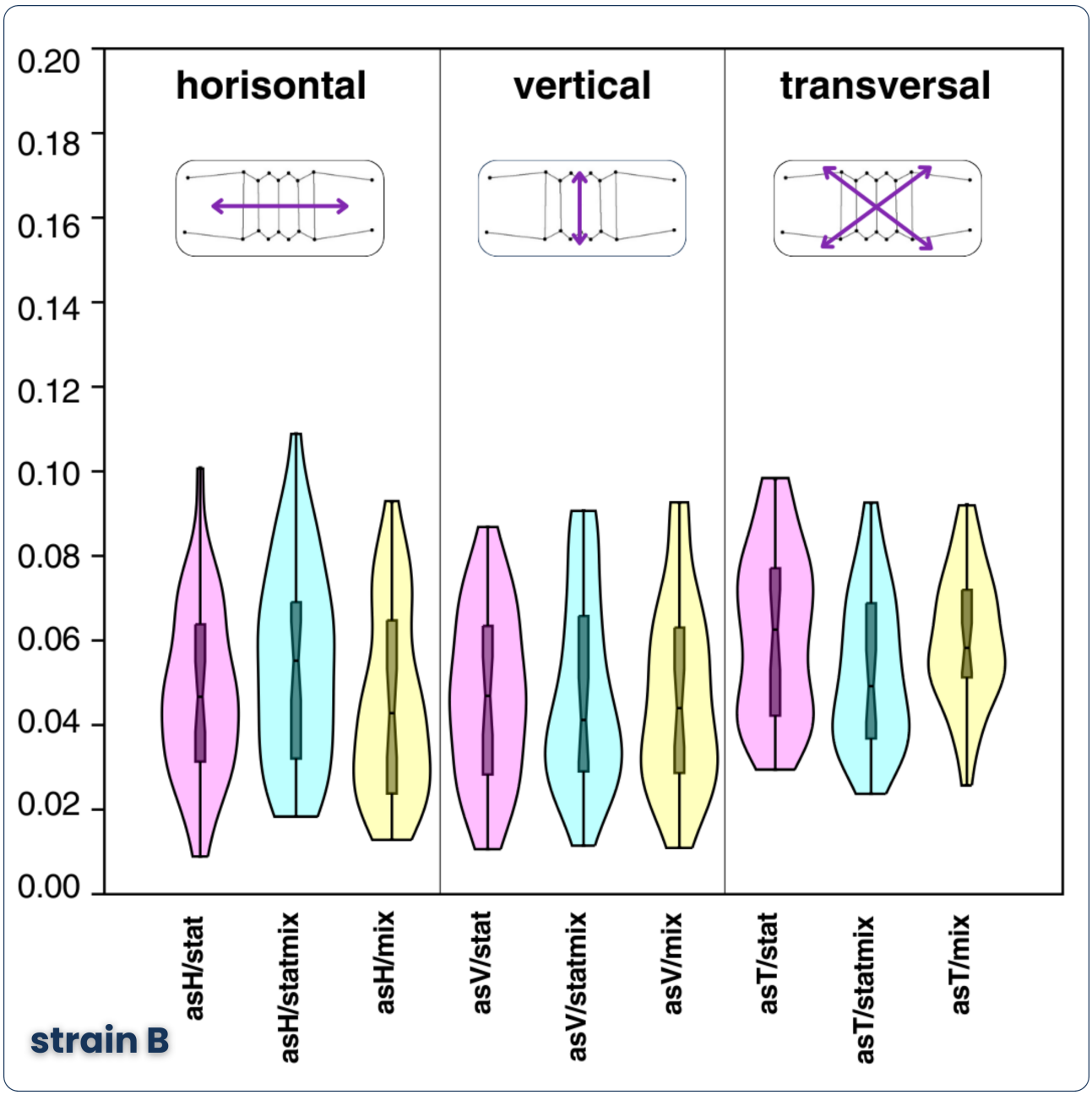

Figure 10. *Graph describing the relationship between treatments and their effect on different types of asymmetry in strain B (spines included). asH = horisontal asymmetry, asV = vertical asymmetry, asT = transversal asymmetry. Stat = stationary treatment, statmix = stationary-mixed treatment, mix = mixed treatment.*

The strain A produced coenobia with relatively low levels of asymmetry in all axes under all three treatments.

The second strain analyzed (strain B) was the river strain (see Fig. 10.). More variability was already evident in strain B, particularly in the degree of asymmetry of the various axes. Across all three treatments, coenobia developed with the greatest degree of asymmetry along the transversal axis. The lowest asymmetry values were observed on the horisontal axis. However, it was a negligible difference compared to the vertical axis as can be seen in Table 3.

It was difficult to identify the treatment that seemed to have the biggest impact on asymmetry in strain B. The horisontal axis was most affected by the stationary-mixed treatment, but asymmetry was high for the stationary treatment as well. The effects of each treatment on the asymmetry of coenobia varied very little along the vertical axis. The mean of the stationary-mixed treatment was

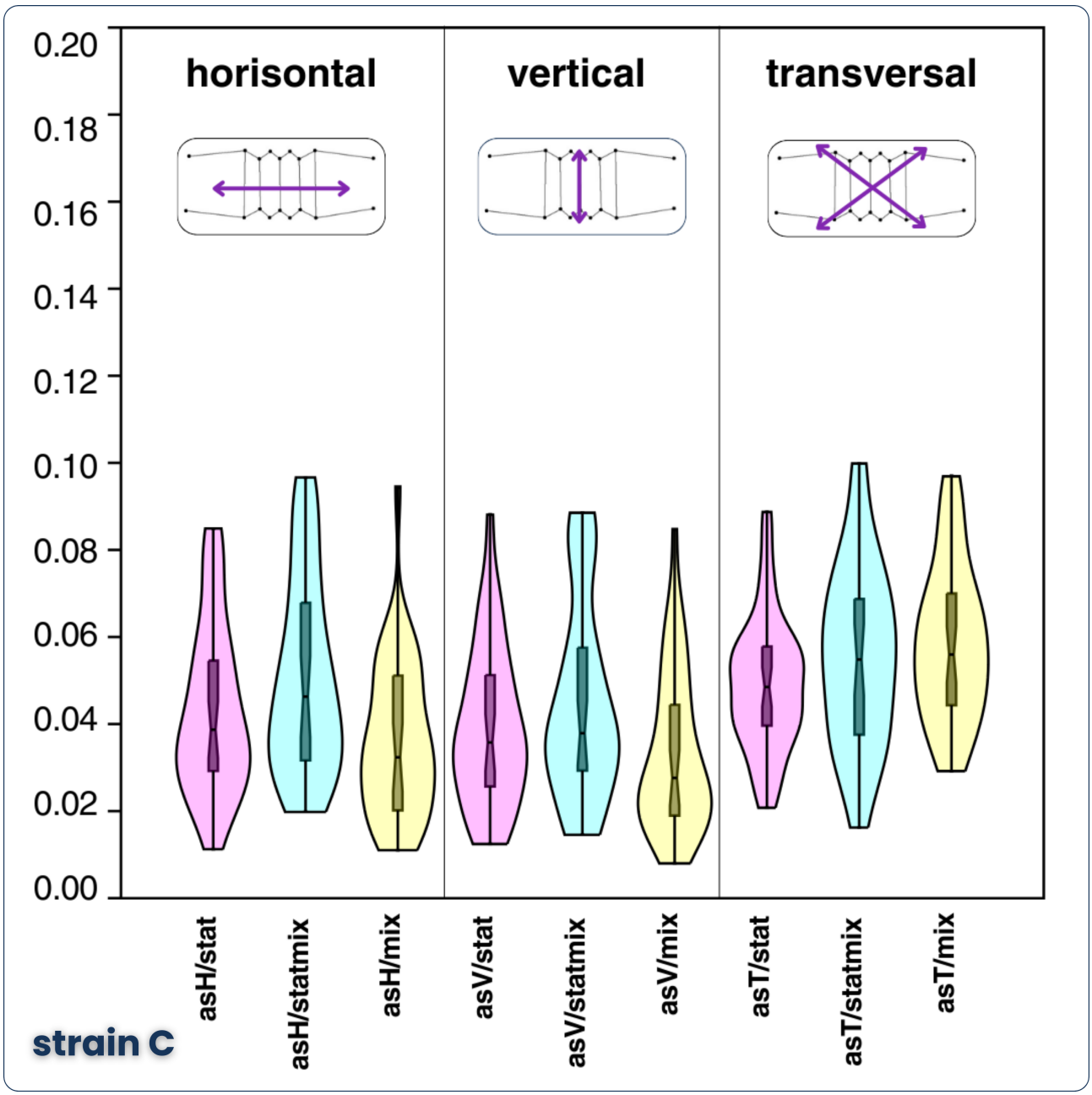

Figure 11. *Graph describing the relationship between treatments and their effect on different types of asymmetry in strain C (spines included). asH = horisontal asymmetry, asV = vertical asymmetry, asT = transversal asymmetry. Stat = stationary treatment, statmix = stationary-mixed treatment, mix = mixed treatment.*

slightly higher than the rest. The median, however, was higher for the stationary treatment. Stationary and mixed treatment caused the highest asymmetry on the transversal axis. For both the stationary and mixed treatments, the mean, median, and their confidence intervals achieved correspondingly high values. The stationary-mixed treatment then had the lowest values.

In general, for strain B, the intervals containing the asymmetry levels broadened. Coenobia grew more asymmetric than in the strain A.

Strain C, taken from the pond, also showed slightly more variability than strain A, especially in terms of the asymmetry axes (see Fig. 11.). The highest level of asymmetry was observed on the transversal axis under all three treatments. The means and medians and their confidence intervals reached higher values than the other axes, as can be observed in Table 3.

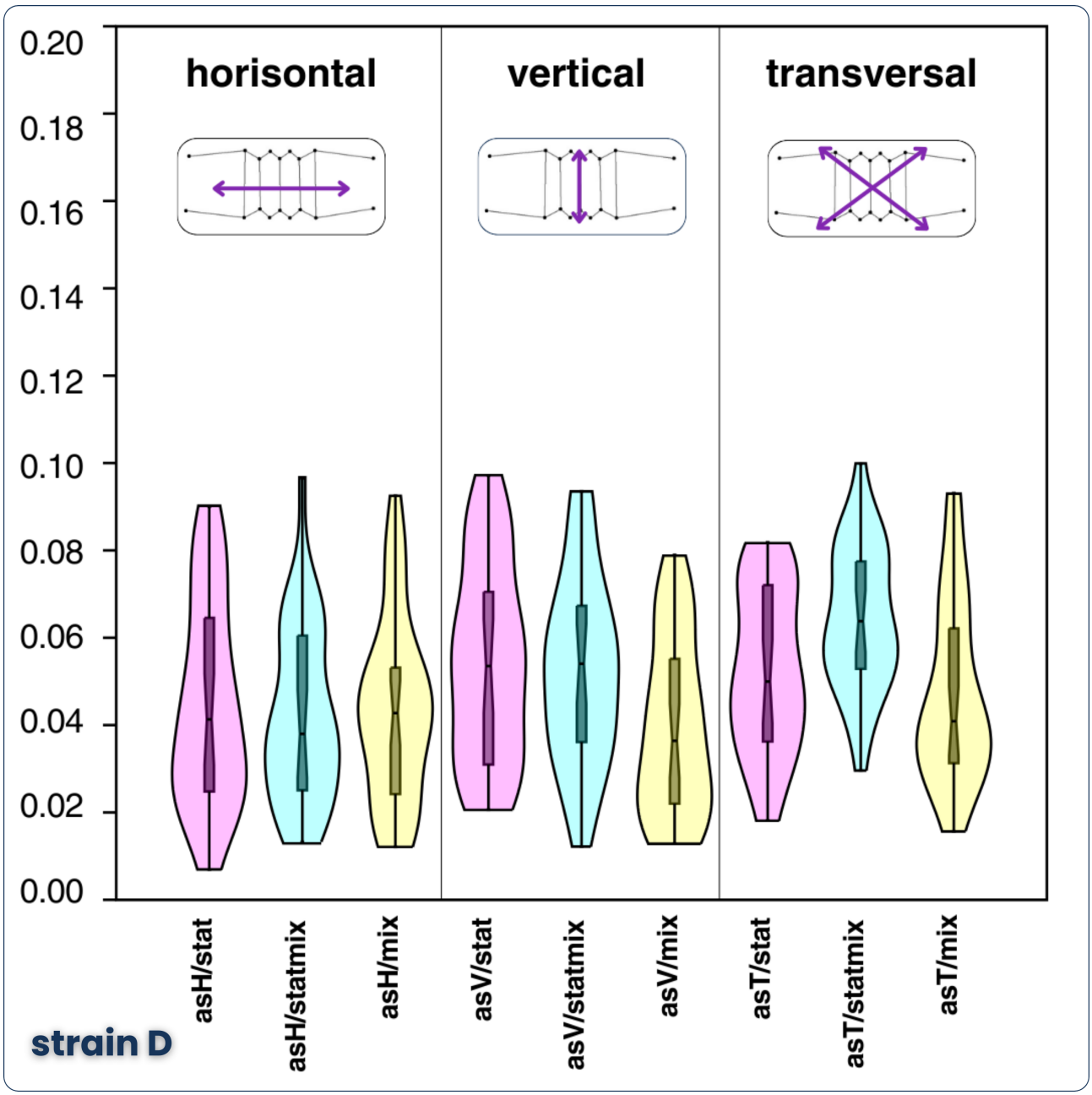

Figure 12. *Graph describing the relationship between treatments and their effect on different types of asymmetry in strain D (spines included). asH = horisontal asymmetry, asV = vertical asymmetry, asT = transversal asymmetry. Stat = stationary treatment, statmix = stationary-mixed treatment, mix = mixed treatment.*

Regarding the treatments and their effect on asymmetry, in all cases the asymmetry was the highest under the stationary-mixed treatment. On the horisontal axis, the second highest asymmetry was due to the stationary treatment, closely followed by the mixed treatment. It may be confirmed that coenobia under the mixed and stationary-mixed treatments did indeed differ in asymmetry, since their confidence intervals of their means did not overlap. Similarly, the confidence intervals of their medians did not overlap, which supported the significance of the results even more robustly. The confidence intervals of the medians also did not overlay for the mixed and stationary treatment, and thus I could be confident that there was a significant difference in asymmetry here as well. On the vertical axis, stationary-mixed treatment caused the highest asymmetry. Under stationary treatment, however, the asymmetry reached relatively high values as well. The lowest asymmetry was observed under the mixed treatment. Confidence intervals for the stationary-mixed and mixed treatments did not

overlap and so the coenobia under these treatments were markedly different in vertical asymmetry. The highest transversal asymmetry was achieved by coenobia under the stationary-mixed treatment. The confidence intervals of the stationary-mixed treatment did overlay the others, but only minimally. The significance of these results is therefore slightly higher.

In strain D, the most asymmetric axis was difficult to determine (see Fig. 12.). It can be said that on the transversal axis the asymmetry reached the highest values and its intervals started at the highest units. However, it could not be considered a striking difference in variability. It was, nevertheless, the only observable variability in the asymmetry of the different axes.

Stationary-mixed treatment had the greatest effect on asymmetry under all treatments in strain D, as can be seen in Table 3. On the transversal axis, the influence of stationary-mixed treatment was most pronounced. The confidence interval of the mean for the stationary-mixed treatment did not overlap with any of the other treatments. Especially the mixed treatment and its confidence interval was very far apart in value from the confidence interval of the stationary-mixed treatment. The same difference was also evident between the stationary-mixed treatment and its confidence interval and the other treatments. Thus, it is certain that the coenobia under the stationary-mixed treatment were indeed significantly different in transversal asymmetry from the other treatments.

	asH				asV				asT			
	mean [PD]	95% CI	median [PD]	95% CI	mean [PD]	95% CI	median [PD]	95% CI	mean [PD]	95% CI	median [PD]	95% CI
Strain A stat	0.04681973	[0.03478028,0.0573284]	0.03413344	[0.02565816,0.03971584]	0.04357205	[0.0349361,0.05123968]	0.03642044	[0.02430396,0.04213367]	0.04479817	[0.03281184,0.05454106]	0.03917696	[0.03449688,0.04875003]
Strain A statmix	0.03870373	[0.0238862,0.04831764]	0.02819852	[0.01658506,0.03357153]	0.05127527	[0.03889303,0.06138028]	0.04049526	[0.02569038,0.04807485]	0.03915146	[0.03298592,0.04452388]	0.03455502	[0.02759492,0.03984303]
Strain A mix	0.05144089	[0.04072918,0.06085419]	0.04195847	[0.02190901,0.05183413]	0.06071604	[0.05081376,0.06993312]	0.05022403	[0.03012841,0.0576227]	0.04308026	[0.03672669,0.04892911]	0.04000486	[0.03546143,0.0458241]
Strain B stat	0.05665643	[0.04169243,0.06867434]	0.0469553	[0.03689926,0.05498192]	0.05661942	[0.04510298,0.06696856]	0.05039513	[0.03851506,0.06132395]	0.07058968	[0.06123339,0.07949775]	0.06717001	[0.05722309,0.078422]
Strain B statmix	0.05967205	[0.04613746,0.06997834]	0.05670351	[0.04802975,0.07021172]	0.07132364	[0.04423568,0.09187485]	0.04650796	[0.02700258,0.05614006]	0.06501207	[0.04923998,0.07684067]	0.054242	[0.04209815,0.06366969]
Strain B mix	0.04802517	[0.03963931,0.05576408]	0.04374686	[0.03607195,0.05577217]	0.062073	[0.04222886,0.0765069]	0.04938224	[0.03843779,0.06274571]	0.07501656	[0.06486852,0.08419827]	0.06694783	[0.0584894,0.07704704]
Strain C stat	0.04448148	[0.03653436,0.05161519]	0.03870675	[0.02946198,0.04629711]	0.04357205	[0.0349361,0.05123968]	0.03642044	[0.02430396,0.04213367]	0.04901808	[0.04430412,0.05363644]	0.04850712	[0.04255497,0.0550682]
Strain C statmix	0.05684826	[0.0440165,0.06726434]	0.04665372	[0.03605979,0.05713765]	0.05453753	[0.04187541,0.06530891]	0.03935723	[0.02437348,0.04345295]	0.06062129	[0.05288566,0.06797953]	0.05913372	[0.0506331,0.06783152]
Strain C mix	0.03767911	[0.03113517,0.04359864]	0.02108189	[0.01270004,0.02516952]	0.0329147	[0.02713346,0.03816816]	0.02761964	[0.01910645,0.03340528]	0.05857635	[0.05303514,0.0638858]	0.05596949	[0.04721071,0.06185343]
Strain D stat	0.05326283	[0.04225355,0.06343205]	0.04285884	[0.02745068,0.05498984]	0.06640717	[0.05351023,0.07793455]	0.05866278	[0.04488523,0.06867019]	0.06074365	[0.05158346,0.06945768]	0.05525492	[0.0424982,0.06378393]
Strain D statmix	0.06828724	[0.04725573,0.0854763]	0.04586821	[0.02713389,0.05525639]	0.08255959	[0.06194206,0.1000117]	0.05933854	[0.03581994,0.06691028]	0.09106301	[0.07003054,0.1078997]	0.07500179	[0.06587117,0.08811636]
Strain D mix	0.04914749	[0.03834927,0.05837573]	0.02588323	[0.01318258,0.03273207]	0.0494145	[0.02917385,0.06251926]	0.03678991	[0.02543697,0.04650898]	0.05006268	[0.04246547,0.05714966]	0.04198705	[0.0293442,0.0477206]

Table 3. *Confidence intervals for the asymmetry data including spines.*

3.1.2 Analysis without spines

The second part of the analysis No. 1. was identical to the first part, but landmarks indicating spines were excluded.

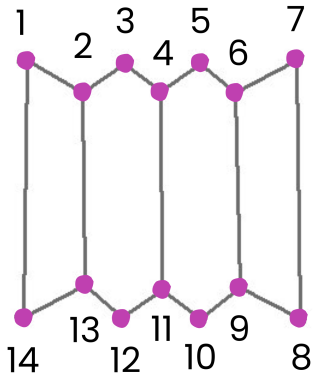

Figure 13. *Layout of landmarks on the coenobium without spines.*

In the analysis of strain A without spines, the axis with the highest degree of asymmetry appeared to be the transversal axis (see Fig. 14). However, it should be noted that this was not a significant variation compared to the other axes. The vertical and horisontal axes then behaved similarly and the asymmetry here was quite low. The vertical axis did however achieve a slightly higher values of asymmetry as can be observed in Table 4.

On the horisontal axis, the greatest asymmetry was formed under the mixed treatment, closely followed by the stationary treatment. On the vertical axis, again, the mixed treatment caused the highest asymmetry. The confidence interval of the median for the mixed treatment did not overlap with the other confidence intervals, therefore the difference in asymmetry could be considered highly significant. On the transversal axis the highest asymmetry was due to the mixed treatment. Stationary and stationary-mixed treatments then produced coenobia of similar asymmetry level.

In strain B, again, the highest level of asymmetry was on the transversal axis (see Fig. 15.). The horisontal axis had the lowest asymmetry level but not very dissimilar to the vertical axis (see Table 4.).

On the horisontal axis, all three treatments produced a similar degree of asymmetry, which was relatively low. The mixed treatment produced coenobia with the lowest asymmetry on the horisontal axis. On the vertical axis, the asymmetry was most pronounced under the stationary-mixed treatment. The confidence interval of the median for this treatment did not overlay the other confidence intervals, thus the difference in asymmetry here was clearly significant. The mixed and stationary treatments had an extremely similar level of asymmetry. Asymmetry on the transversal axis then arose most under the mixed treatment, especially if we focus on the median value. The stationary-mixed treatment then resulted in more asymmetric coenobia than the stationary treatment.

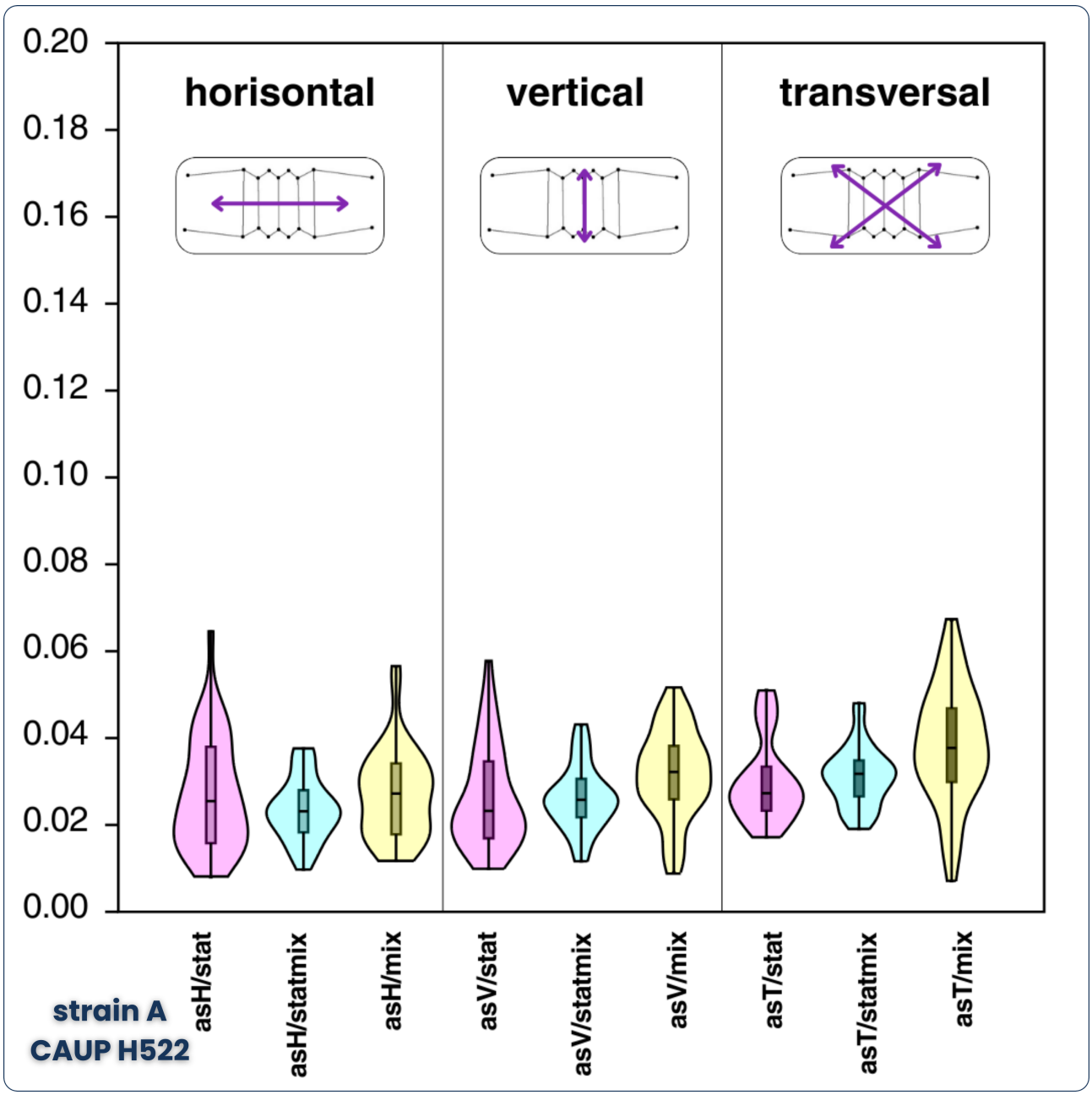

Figure 14. *Graph describing the relationship between treatments and their effect on different types of asymmetry in strain A (spines excluded). asH = horisontal asymmetry, asV = vertical asymmetry, asT = transversal asymmetry. Stat = stationary treatment, statmix = stationary-mixed treatment, mix = mixed treatment.*

Coenobia from strain C produced the highest asymmetry along the transversal axis which was quite high (see Fig. 16.). The horisontal and the vertical axes reached similar levels of asymmetry, which were relatively low.

The mixed treatment had the greatest effect on the asymmetry of the horisontal axis (see Table 4.). However, this was probably due to the effect of only a few outliers. Higher asymmetry was also produced under the stationary-mixed treatment, where again the effect of a few outliers was noticeable. The least horisontally asymmetric coenobia grew under the stationary treatment. The vertical axis was most affected by the stationary-mixed treatment. The stationary and mixed treatment then had a similar effect on the vertical axis, with the mixed treatment reaching slightly higher values. The transversally asymmetric coenobia occurred the most under the mixed treatment. Stationary and stationary-mixed treatment then produced less asymmetry, but still more than on the other axes.

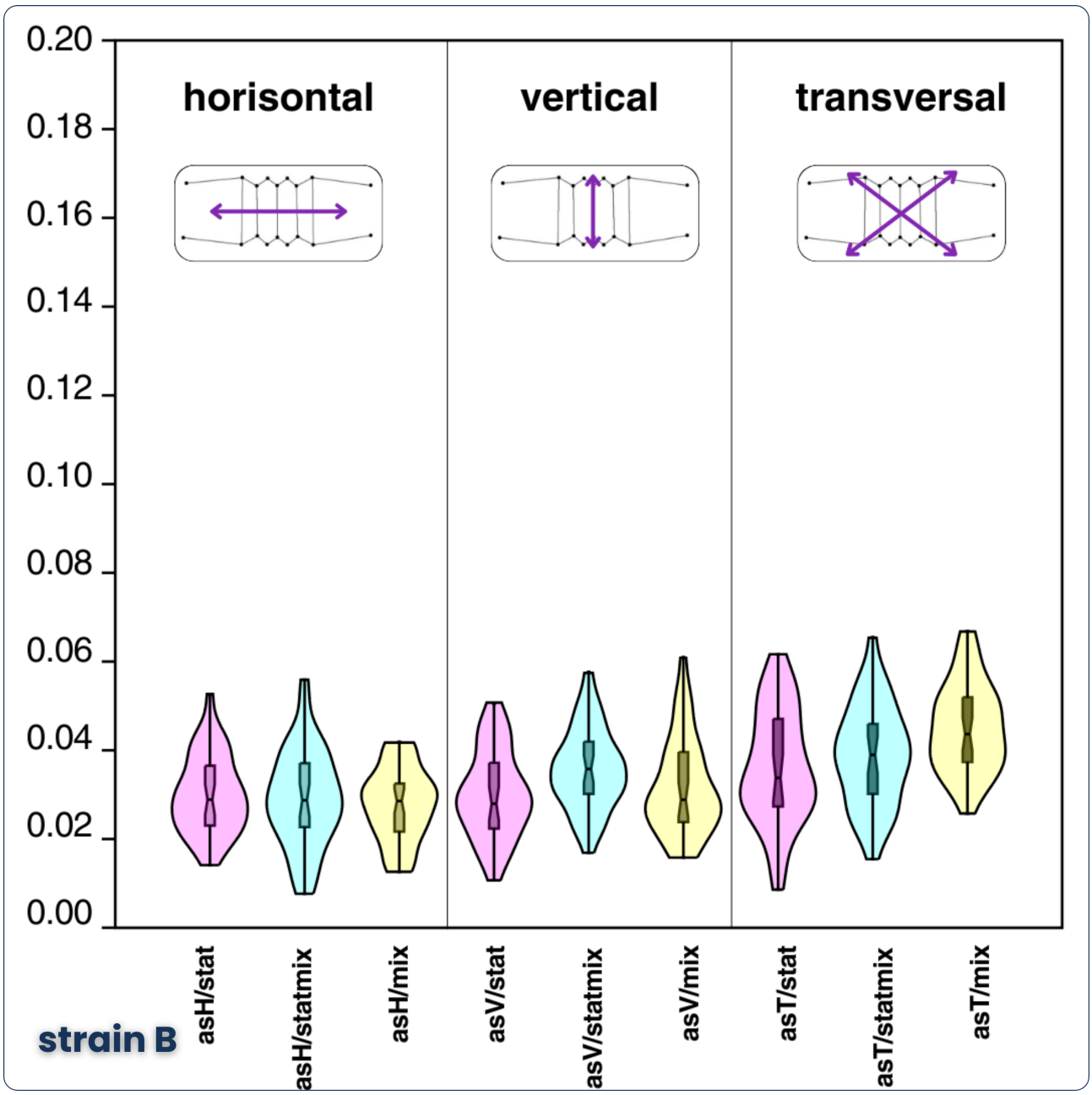

Figure 15. *Graph describing the relationship between treatments and their effect on different types of asymmetry in strain B (spines excluded). asH = horisontal asymmetry, asV = vertical asymmetry, asT = transversal asymmetry. Stat = stationary treatment, statmix = stationary-mixed treatment, mix = mixed treatment.*

Confidence intervals of the mean and median for the stationary and mixed treatments did not overlap. Thus, the two treatments produced coenobia confidently very different in their transversal asymmetry.

Strain D resulted in significantly asymmetric coenobia on the transversal axis. Of the four strains (without spines), the asymmetry here reached the highest values. The horisontal axis was then least asymmetric, especially under the mixed treatment (see Fig.17.).

Most asymmetry on the horisontal axis arose under the stationary-mixed treatment (see Table 4.). However, the difference among the treatments was negligible. The vertical axis was the most asymmetric in the stationary-mixed and stationary treatment. The lowest asymmetry was observed in the mixed treatment. Confidence intervals for the mean and median of the mixed treatment did not overlap with those of the other treatments. Thus, this difference in asymmetry was reliably significant. The transversal axis was extremely asymmetric in all treatments. Nevertheless, the highest asymmetry

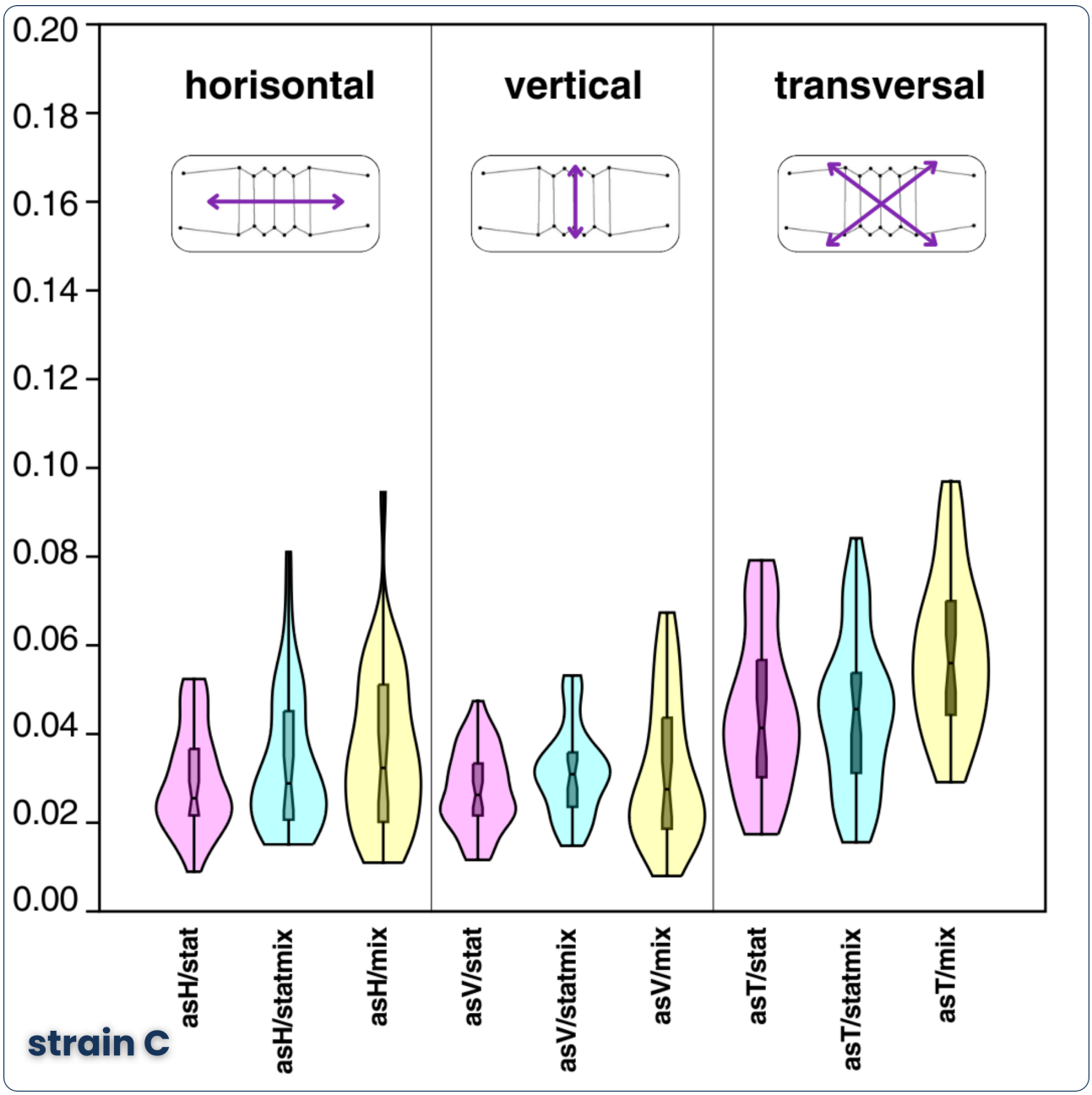

Figure 16. *Graph describing the relationship between treatments and their effect on different types of asymmetry in strain C (spines excluded). asH = horisontal asymmetry, asV = vertical asymmetry, asT = transversal asymmetry. Stat = stationary treatment, statmix = stationary-mixed treatment, mix = mixed treatment.*

was produced under the stationary-mixed treatment. This was followed by the mixed treatment and stationary treatment with much lower values of asymmetry. However, the intervals into which the transversal asymmetry data fell were generally very wide. Thus, the coenobia here produced extremely high asymmetry along the transversal axis in all treatments studied.

A very clearly observable phenomenon in the analysis that did not include spine data was the considerably lower intervals in which the asymmetry data varied than the analysis that did include spines. Thus, this means that spines introduced the highest asymmetry signal into the analysis. When the spines were disregarded, the coenobia became relatively symmetric. The only deviation here was the transversal asymmetry in strain C and D, which was similarly immense as if it included the spine data.

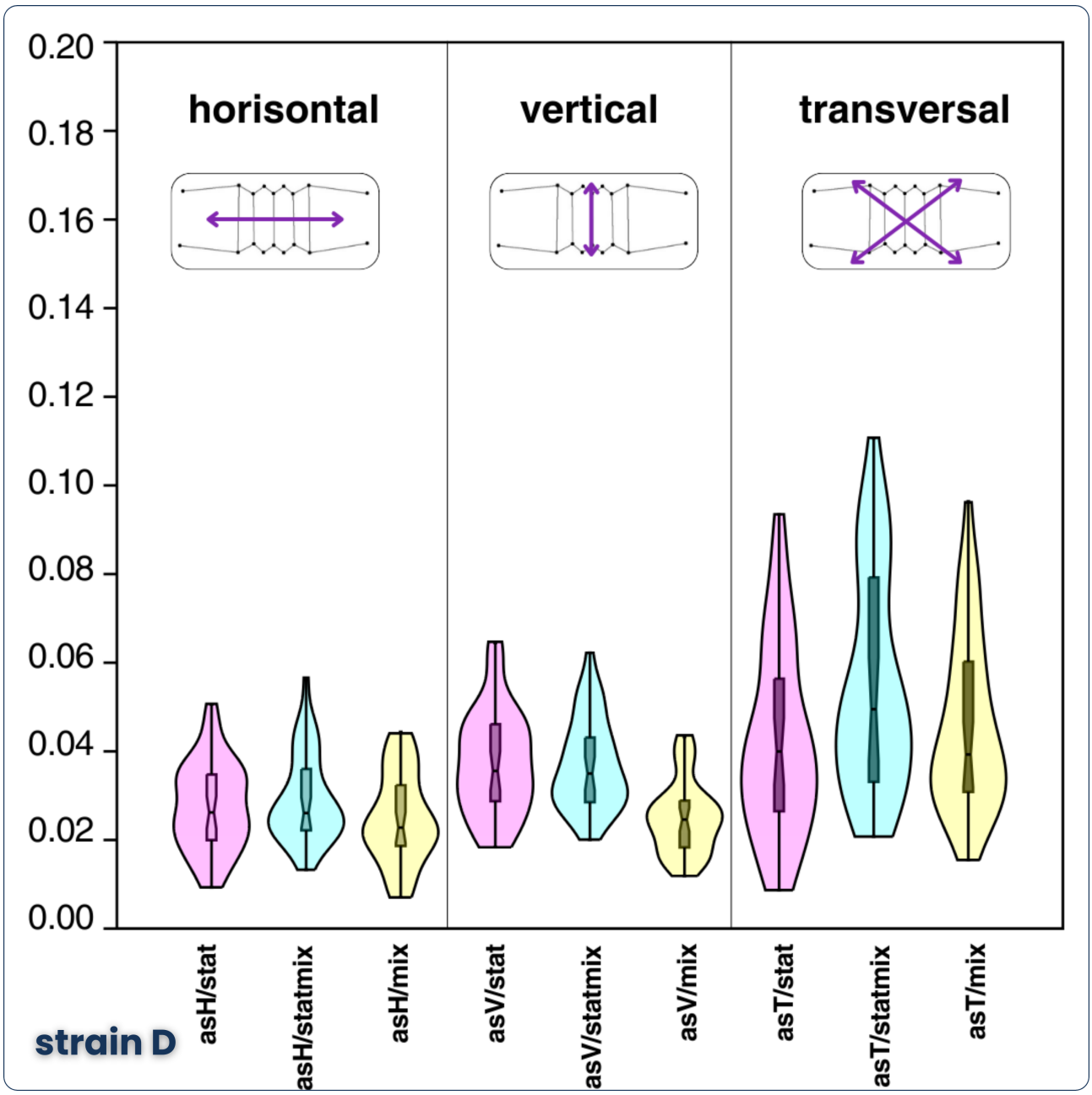

Figure 17. *Graph describing the relationship between treatments and their effect on different types of asymmetry in strain D (spines excluded). asH = horisontal asymmetry, asV = vertical asymmetry, asT = transversal asymmetry. Stat = stationary treatment, statmix = stationary-mixed treatment, mix = mixed treatment.*

	asH				asV				asT			
	mean [PD]	95% CI	median [PD]	95% CI	mean [PD]	95% CI	median [PD]	95% CI	mean [PD]	95% CI	median [PD]	95% CI
Strain A stat	0.02895712	[0.0228619,0.03401823]	0.02600423	[0.02260889,0.03260113]	0.02698034	[0.0229601,0.03075144]	0.02337624	[0.01805539,0.02655896]	0.03547987	[0.02858606,0.04126533]	0.0283642	[0.0245296,0.03052687]
Strain A statmix	0.02600273	[0.0213528,0.02964939]	0.02356843	[0.02172418,0.02571933]	0.02686832	[0.02391816,0.02947927]	0.02580788	[0.02386889,0.02879403]	0.03643842	[0.03206042,0.04031977]	0.03289783	[0.03061915,0.03578974]
Strain A mix	0.03007587	[0.02540468,0.03425582]	0.02786571	[0.0242075,0.03371876]	0.03365753	[0.02949183,0.03751398]	0.03319572	[0.03007568,0.03822231]	0.03924079	[0.03482259,0.04354132]	0.03808586	[0.03037718,0.04261533]
Strain B stat	0.03407968	[0.02425886,0.04023065]	0.02893272	[0.02509341,0.03270684]	0.03115618	[0.02721901,0.03477892]	0.02890765	[0.02509166,0.03110605]	0.04291236	[0.03607096,0.04940758]	0.03746656	[0.02988885,0.04413446]
Strain B statmix	0.03193364	[0.02614176,0.03666393]	0.0293142	[0.02455836,0.03343474]	0.04096289	[0.03382124,0.04662822]	0.03662999	[0.0339632,0.04123103]	0.04617243	[0.03718315,0.05326402]	0.03904793	[0.03258002,0.04140638]
Strain B mix	0.02874915	[0.02563763,0.03161052]	0.02904814	[0.02629971,0.03296125]	0.03163494	[0.0282344,0.03473795]	0.02885505	[0.02440256,0.03138021]	0.0458711	[0.04221378,0.04920075]	0.04409012	[0.03820077,0.04833507]
Strain C stat	0.02949536	[0.02601202,0.03289069]	0.02552552	[0.01794083,0.02775647]	0.02757736	[0.02480064,0.03032224]	0.02626975	[0.02130882,0.03021803]	0.04582014	[0.03990302,0.05165311]	0.04166294	[0.0344345,7,0.04554817]
Strain C statmix	0.03322376	[0.0282029,0.03780617]	0.02886982	[0.02289415,0.03341467]	0.0339825	[0.02962753,0.03786177]	0.03100968	[0.02680272,0.0330269]	0.04879662	[0.04171718,0.0553398]	0.04625026	[0.04065051,0.05492001]
Strain C mix	0.03767911	[0.03113517,0.04359864]	0.03332041	[0.02433286,0.03768341]	0.0329147	[0.02713346,0.03816816]	0.02761964	[0.01910645,0.03340528]	0.05857635	[0.05303514,0.0638858]	0.05596949	[0.04721071,0.06185343]
Strain D stat	0.02742339	[0.024415,0.03038475]	0.02620889	[0.01954448,0.02951015]	0.03892918	[0.03372715,0.04344262]	0.03589254	[0.02942298,0.04010068]	0.04355635	[0.03586349,0.05053991]	0.04049055	[0.03670911,0.05012143]
Strain D statmix	0.03391679	[0.02379497,0.04046805]	0.02673541	[0.02240715,0.03002266]	0.04027779	[0.03373177,0.04542095]	0.03556294	[0.02974153,0.03984996]	0.05779878	[0.04756091,0.06686815]	0.04956884	[0.04070898,0.05748976]
Strain D mix	0.02588217	[0.02220156,0.02939679]	0.02304092	[0.01724319,0.02507489]	0.02483404	[0.02229978,0.02724744]	0.0246141	[0.02262298,0.02775411]	0.0456974	[0.03961286,0.05159236]	0.03929668	[0.02961423,0.04391653]

Table 4. *Confidence intervals for the asymmetry data excluding spines.*

3.2 Analysis No. 2: The relationship between the size of the coenobium and its asymmetry

In the analysis No. 2 I analyzed the asymmetry and variability in relation to the size of the coenobium. This analysis included spines.

After measuring the size of each coenobium, these data were correlated with the asymmetry data. Strains B and D had the lowest Pearson's p value and came out therefore most significant, specifically under the stationary-mixed treatment (See Table 6.).

Strain A			Strain B			Strain C			Strain D		
Stat	Statmix	Mix	Stat	Statmix	Mix	Stat	Statmix	Mix	Stat	Statmix	Mix
4,49571956915069	4,53842177658955	4,08572650958322	3,14127716418374	3,73060391298186	3,4910775159286	4,41864735461481	7,78330906491577	7,42755866875367	3.86845504619667	2,72870848571261	7,76855806726348
3,60256544392712	3,7760958674271	4,49655670732864	2,9943400311625	3,41504921064267	3,404341182797 18	3,66461457727822	1,02382398660881	1,08821323992844	3.64446078925874	2,89826768183264	6,16370244072325
3,84340199418287	4,26896097168594	3,77124500515266	3,87587481164647	3,33057969595551	3,07727512943224	4,18326095554918	1,15275245487582	1,06828629641642	3.97612388025211	3,4068786626797	6,71065156631191
3,53262571530646	3,489821708276 16	3,37128149060396	3,86572474159475	3,16256576567543	3,37402249218611	3,64157856491446	1,03994746127976	8,94411227816626	3.25935661681191	3,41026962114272	6,37763322522984
3,05185280699374	3,6840866499642	4,40761021164279	3,32218134497334	3,53142479901684	3,23694300227854	3,80860575247396	1,14230969725572	1,06384016134422	3.98966512100675	3,43107207087749	5,79360806790073
3,77052972995101	3,73857073105634	3,68963488106283	3,58493762536781	3,29752095436018	4,26387799491913	4,0583035590968	1,14089443469197	9,76609241770275	3.65488181903480	4,15006626453121	7,06216719963182
4,75636474164414	4,56723354145835	5,28995064039144	2,92795909200324	3,52509416737892	3,71987903029117	3,65102192695567	1,13749061046186	1,21057132976312	4.13922832314323	3,67548938540465	6,92718196671634
3,88135428827505	3,67386339188357	3,63256643282527	3,46290019749022	3,83427959335258	3,27815327416045	4,33296216359099	1,00215927986634	9,72140164791066	3.48403182789391	3,21096731704188	6,59425339047399
4,31843400114234	4,01883067570655	5,07451366033129	3,73761807691595	3,03661086666625	3,62591061359457	4,17231883302852	1,03470886941422	1,04968188302721	3.80124687145912	3,44444480286737	6,10024407526271
4,92187859347312	3,64458197572476	3,75324008173087	2,24488515745715	3,08018758447526	3,28725907439956	3,63857878237583	1,11367853929619	9,44644965641119	3.45044361077110	2,97433559340943	6,52482353954666
4,78267823620941	3,86375239337653	3,99033972377179	2,58217500913044	3,42811982806254	3,44760786633283	3,31267682966174	9,99654718168006	1,09527371008347	3.40466183669131	3,56369736213513	6,70798736167894
4,89056801972486	3,54811060832225	4,3547317815095	3,7615961446646	2,85963964318739	3,55771852612192	3,8369468475744	1,01306962029051	8,8550290168293	3.94970111386785	3,63127005636075	7,6064508441483
4,06317951581982	3,91671914858455	4,12698706349102	4,00102000883664	3,22083236308739	4,5380937015937	3,93882244106309	1,15574307506277	9,86568857764683	4.05952720290320	3,35519580485087	5,35815785093679
3,75155967565491	4,23229974258808	3,42532804592819	3,06590932677403	3,79758402730531	3,56094010683196	3,71337073589781	9,98040023690878	9,33781707776383	3.91402747960603	3,55661668193555	7,3375889167431
4,77114824288195	3,85746318481748	4,89223477677749	3,25170382688488	3,47480535026384	3,54070065257021	3,78952357017197	1,00741851062781	8,66809411321517	3.63482308907722	3,59617775484534	7,37095237326147
4,52388107712835	4,13042236204591	4,47535783795863	3,22927408423489	3,31905274304448	3,29388827982978	3,84694756340083	1,31754732151997	1,02628632023968	3.64549341272512	3,33929550121645	8,06194800005281
4,65142869330369	5,32714641143726	3,6479644247778	3,16396463668958	3,69836375231594	3,97847332528446	3,55147934747699	1,20811839467643	1,03870426761208	3.52633032422596	3,11566115687256	6,2783985927057
4,59566704141581	4,53080137625907	4,50741672752316	2,85192527563009	3,49964918876799	3,73626744819538	3,91856337053376	9,48059890278856	1,11386948168186	4.02484782321021	3,5481247003014	8,02101268197753
3,88650943078176	3,73103575134007	4,25172971337026	3,81291810093588	3,53321383445724	3,64611589381236	3,98984683638079	1,13851835977974	1,12689263020041	3.72059732360873	3,45241380936746	7,61525406302669
4,30869469793347	3,95387081787512	3,78975226396426	3,96356181006708	3,63177948425042	3,21873508626534	4,02861156120953	1,20744316636436	1,05186210545341	3.99378545019912	3,85665802361463	7,85264994196934
4,15300025416699	3,1957619505283	3,48078215986644	3,91984977036394	3,50461124805591	3,6284194600098	3,66450921376625	9,34642653043873	1,2641111941246	4.49638620326245	3,71225672603606	9,09901246167834
3,71880879972188	4,70432307091632	4,25781373216088	3,26268209368373	3,36988130354765	3,06903260183256	3,63716770150744	1,08373800134329	1,12074303229797	3.51915551738703	2,79387624000142	6,83947934990506
4,82556444597129	4,44276440468719	3,74526441730828	3,33187968303512	3,45389072078303	3,46561682821399	4,03098071882706	7,4342981436642	9,95056782299382	3.69204851298330	3,67484617969847	7,33442416129431
4,90466501291259	4,07129859163169	3,70381260025096	3,76328240296213	4,02050439068975	2,73950624099388	3,69158803527997	1,2646182120396	1,20587114660822	3.75870323382946	3,56917668688764	7,383784410600 18
5,46250451309247	4,23299276845328	3,96259454846891	3,21549546899247	4,2490711403265	4,34972349057322	3,82438085039773	1,18481133050325	1,01646894252166	4.20051319615962	3,78397571638908	8,39932669259203
4,83910517439835	3,95633739152206	3,6314008622324	3,19863165188561	3,73327083281017	2,89995498049347	3,86371223336084	1,04145704557499	9,94358531360238	3.66535127920913	4,08789065411491	7,50047739221385
4,62825681127475	4,40514913355824	3,07707292370164	3,79560271893674	3,6509846464877	3,16895180707368	3,60606356633441	1,03971002901984	9,99628069722823	4.24839119876899	3,90205145475499	7,50058960645391
4,00034859592122	3,10327157117202	4,34803723279571	3,48941335406907	2,60402679624376	3,26459628268012	4,01482599595272	1,04641220367501	1,12807990753216	4.26668619787196	3,70785652365352	7,21342151825332
5,57334379983068	4,3183690336875	3,69310318175801	3,27177491755028	3,3397421723507	3,85968910665095	3,54485856166677	1,26686544492916	1,07459770250184	3.46257771673712	4,09763956443219	7,24043008237617
3,14803024833696	4,54357543986867	2,53929233361493	3,5688568042006	3,53602727490738	3,38229130094444	3,92765974991611	1,16847633456756	9,61732031285222	3.05039523850781	3,8211989101735	6,68842366414622
6,04160252839519	4,28981222070254	3,08428363733875	3,16394619985163	3,50771609772259	4,45326409626816	3,8228973886889	1,22970448121128	1,18933774756281	4.06350765280988	3,5423007275561	6,74173980182828
4,59307510159467	3,76226734238219	3,43296519061875	3,47345329287408	3,52388122513925	3,18401912333732	3,78914898097185	1,16675985342124	1,31839355108995	4.20064942069147	3,69279177738349	8,52766120079565
4,49647600369922	3,97417636470474	3,34142517830674	3,47264708511789	3,10683297122827	3,67597077125364	3,84649118606093	1,0174391873719	9,68614847203068	3.88962580319610	3,53296932087192	7,25910041870815
4,28491669826977	3,83486346272951	3,65788721653482	2,90732217379193	3,74363756555335	3,48700842811969	4,00385924938538	6,86481245191739	9,17839976369641	3.82304706862064	4,12773612959399	9,11108512868924
3,49251739835005	4,16418325992291	4,17368076296105	3,80979804072488	3,79203624572457	2,59435819509266	4,60755237505651	1,03638723457982	1,14428570635911	3.87048733652782	3,39585695288309	6,95306966582227
3,55212690589111	3,44759900349343	3,22757735082454	3,68058947573468	3,41386063635358	3,48086276022993	3,55730859561614	9,7754366199731	1,24114337966606	3.60578316350585	3,73416954920665	7,34304962381283
3,98103350623651	4,18706606375183	4,10022289367027	3,4276554993497	3,62603854854793	3,29731624877634	3,44386733516583	8,59783564496192	1,01413907111183	3.71434905318400	3,91715387040699	7,76582756554495
4,26492216940838	3,98930932479407	4,33915826450758	2,71468946454081	3,71276252345279	3,53714024476145	3,50812548869684	1,23450525402779	8,54260498911193	3.63046216831350	3,75085175512028	7,56909689314239
3,73448642906744	4,03582636450634	3,80757797031131	3,4151362426052	2,3186801801408	3,48140855912597	3,72542018510068	1,09045497640001	8,96166806149639	3.78653829007739	3,70629044853326	6,64691616047957
3,94758294543777	4,02661285836013	4,31386202324038	3,29798760189031	3,25819053395524	3,23786280678406	3,59722114972099	1,03206486660911	9,38774200753302	3.33258324893934	3,65029831353244	7,69195431025894

Table 5. *Sizes of 40 coenobia from each strain and treatment in µm.*

Nevertheless, a negative correlation was also observed for other strains and treatments. For example, strain B had a negative correlation for all data evaluated. However, some values were noticeably close to zero and so could not be classified as significant. The same was true for the entire strain D. A positive correlation was then observed for strain B under the stationary treatment and specifically on the transversal axis. However, the value was not very high (0.088688) and could be considered an insignificant positive correlation. Other data for strain C also showed negative correlations between values, but not all were significant. The most positive correlations observed were achieved by strain A. For the stationary-mixed treatment, both the vertical and transversal axes reached positive values. That is, the larger the coenobia were, the more asymmetric they were.

Strain A

	Stationary			Stationary-mixed			Mixed		
	Horisontal	Vertical	Transversal	Horisontal	Vertical	Transversal	Horisontal	Vertical	Transversal
Slope a	-9.8462E-05	-2.2933E-05	-0.00015008	-0.00019835	0.00013376	4.007E-05	1.171E-05	-0.00010964	-4.4333E-05
Confidence interval	(-0.00025206, 2.1453E-05)	(-0.00030796, 0.00014453)	(-0.00028072, -2.968E-06)	(-0.0004916, 0.00034779)	(-0.00032221, 0.00071187)	(-0.00010513, 0.00024976)	(-0.00017026, 0.00016288)	(-0.00031745, 3.4728E-05)	(-0.00015174, 5.0775E-05)
r	-0.17433	-0.015835	-0.27233	-0.20314	0.153	0.089516	0.020036	-0.19445	-0.12275
Permutation p	0.2874	0.9317	0.0882	0.1766	0.3334	0.5784	0.9056	0.2296	0.4539

Strain B

	Stationary			Stationary-mixed			Mixed		
	Horisontal	Vertical	Transversal	Horisontal	Vertical	Transversal	Horisontal	Vertical	Transversal
Slope a	-0.00014784	-9.2447E-05	-0.00011327	-0.00046544	-0.0010759	-0.0005334	-0.00018605	-0.00033396	-0.00021526
Confidence interval	(-0.00038957, 5.6453E-05)	(-0.00026579, 8.4217E-05)	(-0.00034091, 0.00012319)	(-0.001147, 0.00017796)	(-0.0022131, 7.4869E-05)	(-0.001246, 0.00016475)	(-0.00036033, 6.6926E-05)	(-0.0006604, 0.00015326)	(-0.00044233, 3.4853E-05)
r	-0.12514	-0.097891	-0.14408	-0.41319	-0.47809	-0.41139	-0.29249	-0.24022	-0.28125
Permutation p	0.4454	0.5428	0.372	0.0199	0.0077	0.0209	0.0678	0.1451	0.0785

Strain C

	Stationary			Stationary-mixed			Mixed		
	Horisontal	Vertical	Transversal	Horisontal	Vertical	Transversal	Horisontal	Vertical	Transversal
Slope a	-0.00028885	-0.00026297	5.0464E-05	-7.608E-05	-2.6165E-05	-1.0983E-05	-3.8762E-05	-4.6505E-06	-7.5429E-06
Confidence interval	(-0.00064096, 0.0001182)	(-0.00050611, 0.00010939)	(-0.00012981, 0.00026867)	(-0.00014525, 1.6784E-05)	(-0.00011212, 4.1918E-05)	(-5.611E-05, 4.5284E-05)	(-8.5204E-05, 1.9722E-05)	(-5.2211E-05, 3.8167E-05)	(-5.0619E-05, 4.0417E-05)
r	-0.31212	-0.26328	0.088688	-0.27443	-0.093531	-0.061644	-0.23213	-0.031521	-0.051885
Permutation p	0.0484	0.0974	0.5859	0.0874	0.5631	0.7029	0.1458	0.8448	0.7478

Strain D

	Stationary			Stationary-mixed			Mixed		
	Horisontal	Vertical	Transversal	Horisontal	Vertical	Transversal	Horisontal	Vertical	Transversal
Slope a	-0.00049883	-0.00041724	-0.00051279	-0.0011798	-0.00070281	-0.00066069	-2.3272E-05	-0.00031884	-9.8385E-05
Confidence interval	(-0.00083979, -0.00020017)	(-0.00087202, 0.00014162)	(-0.00084297, -0.00020123)	(-0.0018507, -0.00038183)	(-0.0015542, -4.0805E-05)	(-0.001188, -6.5449E-05)	(-0.00011119, 9.4493E-05)	(-0.00060801, 9.4539E-05)	(-0.00019141, -2.8792E-05)
r	-0.43162	-0.31875	-0.53194	-0.6314	-0.37805	-0.35651	-0.057329	-0.45233	-0.33039
Permutation p	0.52	0.0456	0.03	0.01	0.0176	0.0233	0.7258	0.27	0.37

Table 6. *A table representing the correlation analysis of size and asymmetry of coenobia.*

Specifically, the vertical axis, which had a value of 0.153 was very deviated from the other values. In the mixed treatment, a positive correlation was observed on the horisontal axis, but it was a value close to zero (0.020036) and therefore, again, could not be classified as significant.

In morphospace, I then chose to visualize the two most significant strains B and D, particularly under the stationary-mixed treatment. Using multivariate regression, I observed how the shape of coenobia changed from the minimum to the maximum size. As a control, I also visualized the average coenobium size. A coenobium of average size represented the most ideally symmetric individual (See Fig. 18. and 19.).

For both strains B and D, the results obtained by correlation analysis could be confirmed after visualization. The top image shows the coenobium with the smallest size (Min.). The middle image shows the coenobium of average size and the bottom image shows the coenobium of the largest size (Max.). These images are not representations of the specific coenobia studied, but images produced by averaging all coenobia.

Visualization of the correlation analysis for strain B showed that the coenobium of the smallest size was significantly more asymmetric than the coenobium of the largest size. In the smallest coenobium, a significant leftward skew could be observed. The left spines were shorter and open to a wider angle than on the right side. The entire core of the coenobium then leaned to the left. The asymmetry was observable on the morphospace grid, which was heavily deformed. The image representing the largest coenobium was then quite symmetric when compared to the highly symmetric average coenobium. There was a noticeable slight rightward skew, but the grid was only minimally deformed.

Visualization of the correlation analysis for strain D again confirmed a high degree of asymmetry of the smallest coenobia. This time the deformation was quite different from that observed for strain B. On both sides, the spines curved inwards. On the right side, they intersected. This caused an extreme deformation of the morphospace grid on both sides. The core of the coenobium then tilted slightly to the right, but the grid remained relatively intact. As for the largest coenobium, there was a noticeable shape difference from the average coenobium. The spines here opened to a wider angle, which also deformed the grid slightly. However, it was still a very symmetric and functional shape compared to the coenobium of the smallest size.

All the shape deformations observed were located mainly in the spine region. The shape of coenobia cores changed only minimally.

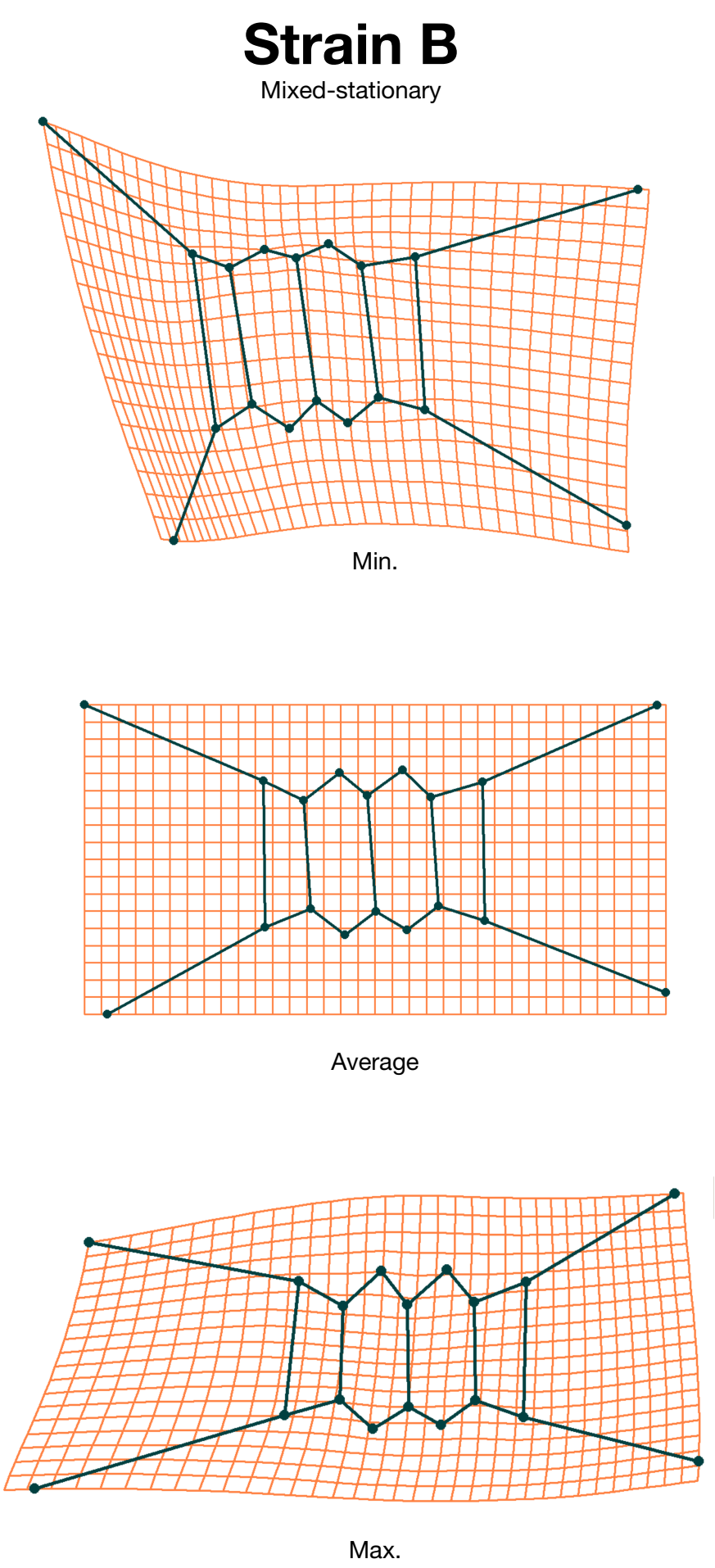

Figure 18. *A visual representation of the relationship between the size and the asymmetry of coenobia in morphospace for strain B.*

Strain D

Mixed-stationary

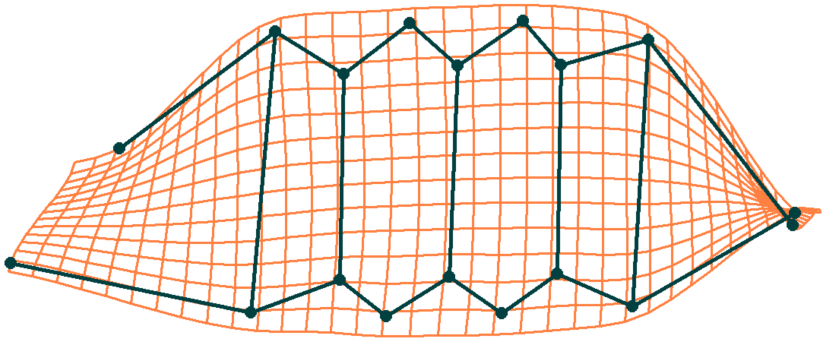

Min.

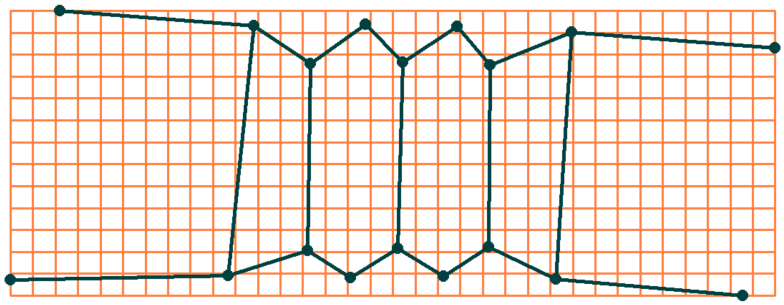

Average

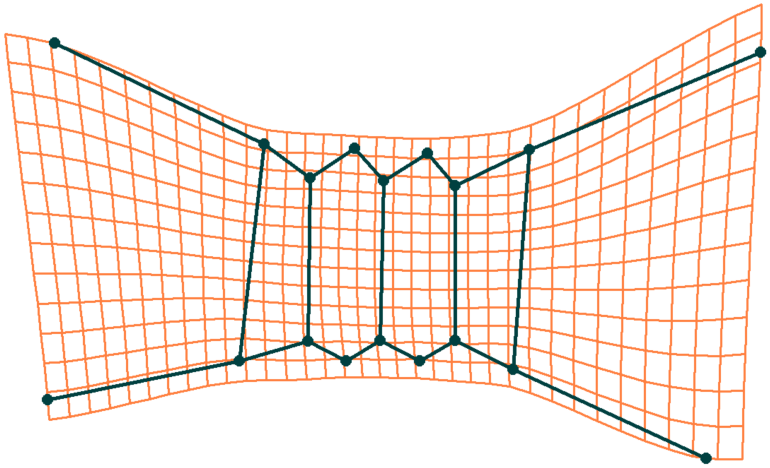

Max.

Figure 19. *A visual representation of the relationship between the size and the asymmetry of coenobia in morphospace for strain D.*

3.3 Analysis No. 3: Analysis of symmetric and asymmetric variability within the morphospaces of individual strains

Analysis No. 3 was designed to provide a more detailed description of the symmetric and asymmetric variability among the four strains. PCA (RWA) was performed on all strains. A symmetric variation, which aims to keep all regions of the coenobium identical to each other, was described. Three types of asymmetry were also presented. Horisontal asymmetry divides the object into two horisontal segments. Vertical asymmetry divides the object into two vertical segments and transversal asymmetry divides the object into two transversal segments.

3.3.1 Strain A

The spines of the consensus coenobium shape extended horisontally from the core of the coenobium, whose cells were all relatively equal in size. The entire right side of the coenobium angled slightly upwards (see Fig. 20).

For strain A, symmetric variation accounted for 68.24% of all variability. Symmetric variation corresponded to components PC1, PC3 and PC7. PC1, which accounted for 51.29% of the variability of all subspaces, mainly described changes in spine shape. On one margin of the morphospace spectrum the spines opened wide and then crossed each other on the other margin of the spectrum. PC3, which accounted for 9.01% of all variability, on the other hand, described changes in the shape of the coenobium core, the spines here remained symmetric. On one margin of the morphospace spectrum, the entire core was enlarged. On the other margin, the cells were shrunken. The same was observed for PC7, describing 2.87% of all variability, which showed deformations of the coenobium core, not the spines. In this case, on one margin of the spectrum, the cells were extremely narrow and on the other margin the cells widened.

Horisontal asymmetry in strain A corresponded to 9.40% of all variability. Horisontal asymmetry represented components PC2 and PC5. PC2, which accounted for 13.62% of all variability among all subspaces, described changes in spine shape. One spine in a segment opens wide and the other then points inwards and crosses the other segment. PC5, describing 3.80% of the variability, again illustrated changes in spine shape. Within a segment, the spines are of different lengths. Otherwise, the two segments are relatively symmetric in comparison to the consensus. A slight deformation of the coenobium core could also be observed.

Vertical asymmetry in strain A accounted for 15.69% of all variability and corresponded to PC4 and PC8 components. PC4, corresponding to 6.62% of all variability, again described spine deformations. Within both vertical segments, the spines bent in the same direction and angle. PC8, which described 2.22% of the variability, showed changes in spine shape as well. This time, however,

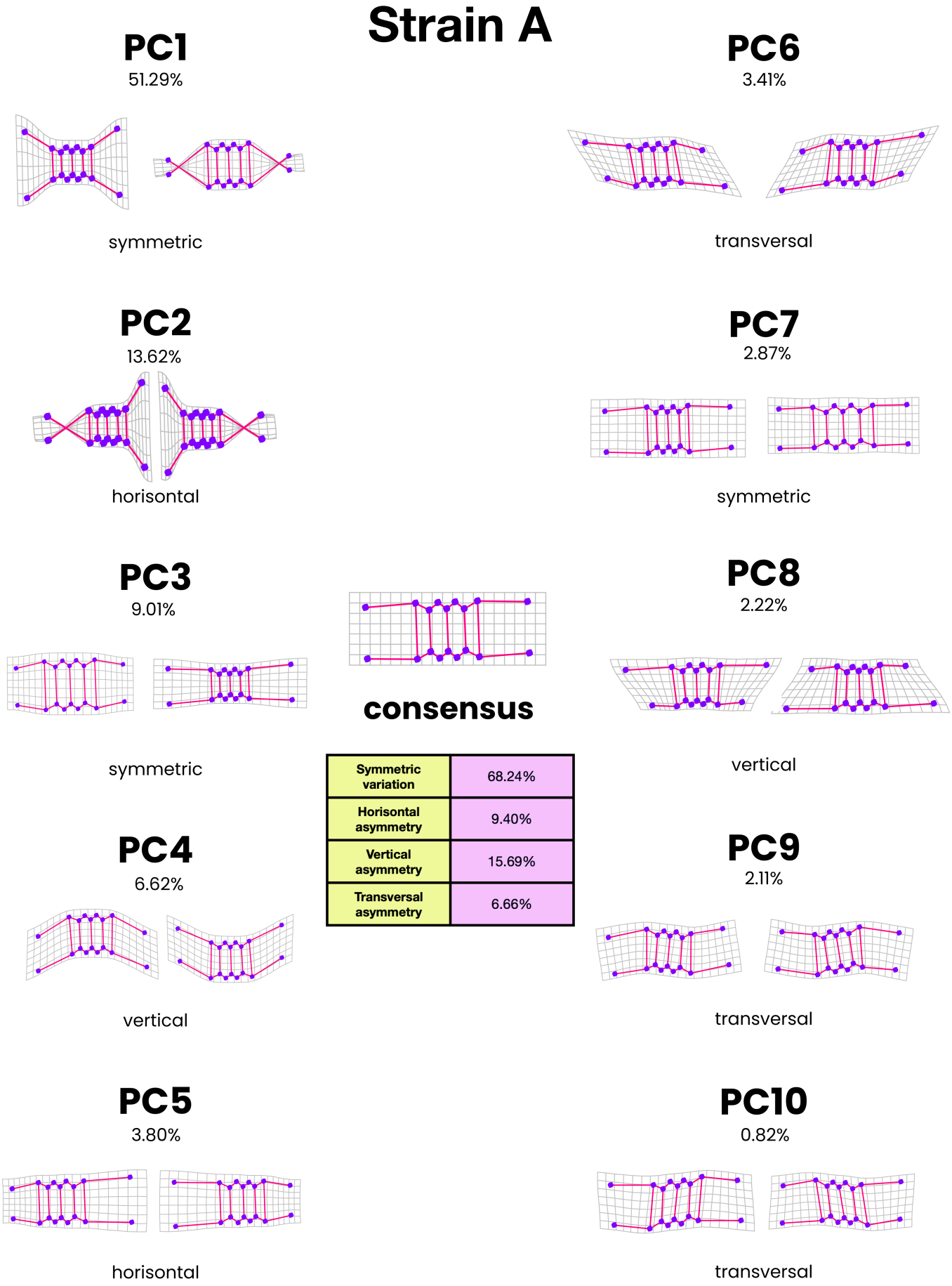

Figure 20. ***Strain A:*** *A scheme showing Desmodesmus communis coenobia reconstructed by principal component analysis of biradial symmetry. The first ten principal components are illustrated. These configurations represent the most peripheral positions that the shapes assume in morphospace. The configuration of the consensus coenobium is illustrated in the middle. A table showing the relative amounts of symmetry variation and the three types of asymmetry are also shown.*

the spines were of different length within a segment. Otherwise, however, the spines were relatively symmetric.

Transversal asymmetry in strain A was responsible for 6.66% of all variability. Transversal asymmetry corresponded to components PC6, PC9 and PC10. PC6, corresponding to 4.99% of all asymmetry, mainly described the deformation of the spines. One spine was always longer within a segment. The spines then bent slightly towards each other. Slight deformation was also observed on the core of the coenobium. PC9, corresponding to 2.11% of all variability, again described mainly deformations of the spines. The spines bent in the same direction within the segment. The core of the coenobium was also slightly deformed. PC10, accounted for 0.82% of all variability and described deformation of both the spines and the core. The spines were bent in the same direction within the transversal segment. The core of the coenobium was also deflected.

3.3.2 Strain B

The spines of the consensus coenobium in strain B extended transversally from the core of the coenobium. The core of the coenobium had middle cells larger than the marginal cells (see Fig. 21).

Symmetric variation accounted for 69.39% of all variation in strain B and corresponded to components PC1, PC4 and PC7. PC1, which accounted for 56.45% of all variation among all subspaces, described deformations of both the spines and the core of the coenobium. On one margin of the morphospace spectrum, the spines opened extremely wide, and on the other side of the spectrum they then converged to close proximity. The core of the coenobium was higher than broader on one margin of the spectrum and broader than higher on the other side of the spectrum. The PC4 described 5.69% of total variability and showed the deformation of the coenobium core resulting in deformation of the spines. The coenobium core was very short on one margin of the spectrum and the spines were long. On the other margin of the spectrum, the core was much larger overall but the spines were shorter. PC7, corresponding to 3.67% of all variability, described the shape changes in the coenobium core. The coenobium was much wider and more extended on one margin of the spectrum and then much narrower on the other margin of the morhospace spectrum.

Horisontal asymmetry together accounted for 7.69% of the variability and it corresponded to PC3 and PC5 components. PC3 accounted for 7.58% of the variability of all subspaces. This component described the deformation of the spines. Here, one spine within the segment emerged horisontally from the coenobium core and the other was deflected outwards, when compared to the consensual coenobium. The coenobium core remained very symmetric. Component PC5 accounted for 5.32% of all variability. This component again described changes in spine symmetry. This time, one spine in the horisontal segment was very short and was directed horisontally from the coenobium core. The other spine then curved outwards and was much longer.

Vertical asymmetry in strain B accounted for 11.81% of all variability and described components PC6 and PC9. PC6 then described 4.99% of all variability and again described mainly spine asymmetry. One spine within the vertical segment deflected outwards. The other spine was then

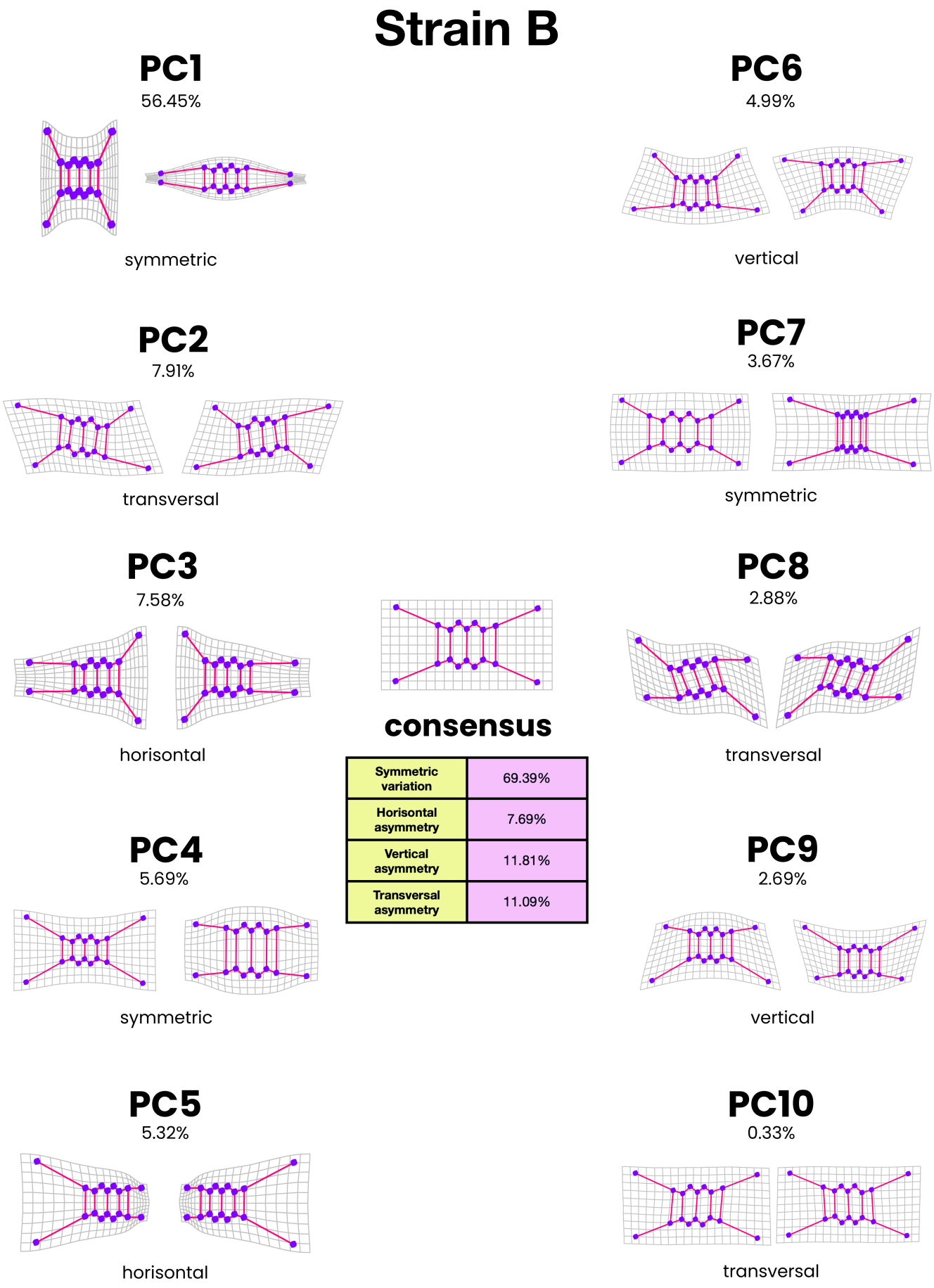

Figure 21. ***Strain B:*** *A scheme showing Desmodesmus communis coenobia reconstructed by principal component analysis of biradial symmetry. The first ten principal components are illustrated. These configurations represent the most peripheral positions that the shapes assume in morphospace. The configuration of the consensus coenobium is illustrated in the middle. A table showing the relative amounts of symmetry variation and the three types of asymmetry are also shown.*

relatively symmetric when compared to the consensual coenobium. PC9 accounted for 2.69% of all variability. This component again described changes in spine shape. This time, one spine within the segment was significantly shorter than the other but otherwise they both emerged symmetrically from the coenobium core, as was the case for consensus. For both PC6 and PC9 components, the coenobium core was very symmetric.

Transversal asymmetry accounted for 11.09% of all variability, similar to vertical symmetry. Transversal asymmetry then corresponded to components PC2, PC8 and PC10. The PC2 component described 7.91% of all variability. It was represented mainly by the deformation of the spines, but also partly by the deformation of the core. One spine within the segment was shorter and more deflected. The whole coenobium then twisted in a spiral manner and this slightly deformed the coenobium core. The PC8 component described 2.88% of the variability. The whole coenobium twisted spirally, which deformed mainly the spines but slight deformation was observed on the core as well. One spine within the segment was shorter than the other. PC10 corresponded to 0.33% of all variability of all subspaces. In this component, the entire coenobium was relatively transversally symmetric, but moderate shape changes were observable in the coenobium core, which was slightly skewed.

3.3.3 Strain C

The spines of the consensus coenobium shape in strain C emerged slightly transversally from the core of the coenobium. The coenobium cells were all relatively equal in size. The entire coenobium was deflected upwards on the right side (see Fig. 22).

The symmetric variation accounted for 47.57% of total variability and corresponded to components PC1, PC5 and PC9. PC1 accounted for 38.71% of all variability and represented asymmetry of the spines. On one margin of the morphospace spectrum, the spines converged horisontally. At the other edge of the mophospace spectrum, the spines were transversally deflected outwards. The entire coenobium was slightly turned upwards on the right side. PC5 explained 4.26% of all variability from all subspaces and described the asymmetry of the coenobium core. On one margin of the morphospace spectrum, cells were much more expanded than the cells on the other margin. This also caused a change in spine length on both margins of the spectrum. The entire coenobium was slightly skewed upwards on the right side. PC9 accounted for 2.46% of all variability. The PC9 component described a slight deformation of the coenobium core. Cells were again more extended on one side of the morphospace than on the other. This time, however, the differences were subtle. The coenobium was slightly tilted upwards on the right side.

Horisontal asymmetry accounted for 16.86% of all variability and described components PC4 and PC7. The PC4 component was responsible for 10.67% of all variability and described the deformation of spine symmetry. One spine here was slightly shorter within the horisontal segment and emerged horisontally from the coenobium core. The longer spine then skewed upwards. The cell from which the shorter spines emerged was smaller than the rest. The PC7 component described 3.63% of all variability and again described spine shape changes. The spines differed primarily in length within the segment, but their direction was relatively the same. In contrast to PC4, the smallest cell was the one from which the longer spines emerged. For both components PC4 and PC7, the coenobia were

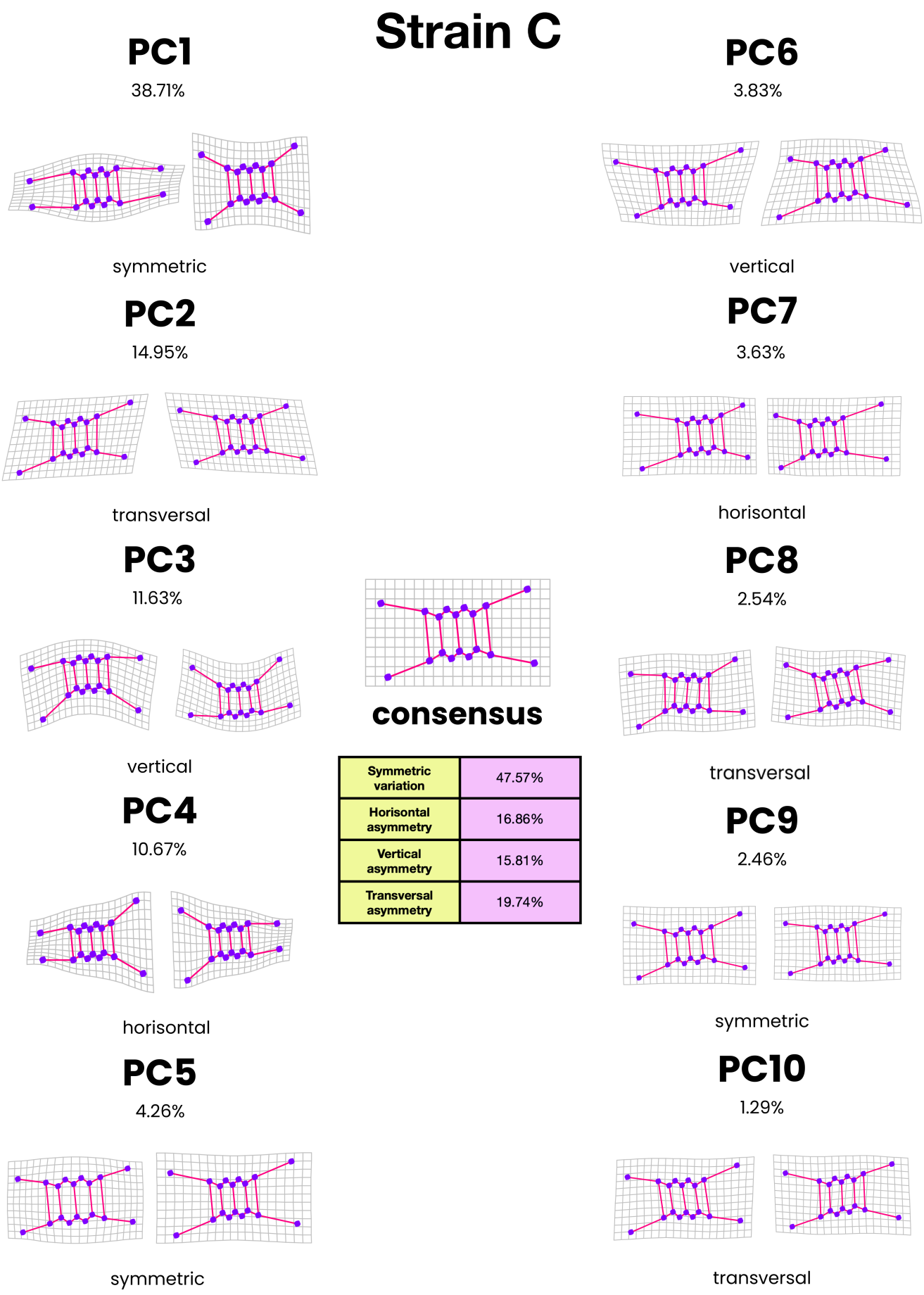

Figure 22. ***Strain C:*** *A scheme showing Desmodesmus communis coenobia reconstructed by principal component analysis of biradial symmetry. The first ten principal components are illustrated. These configurations represent the most peripheral positions that the shapes assume in morphospace. The configuration of the consensus coenobium is illustrated in the middle. A table showing the relative amounts of symmetry variation and the three types of asymmetry are also shown.*

upwardly directed on the right side.

Vertical asymmetry together accounted for 15.81% of the variability and was reflected in the components PC3 and PC6. PC3 accounted for 11.63% of the variability. This component was indicative of the spines deformation, which both turned in the same direction within the segment. However, one of the spines was deflected more significantly and was slightly longer. PC6 then described 3.83% of the variability and explained the asymmetry of the spines as well. The direction of the spines here was relatively symmetric within the horisontal segment and spines differed only in length. Coenobia from both PC3 and PC6 components again skewed upwards on the right side.

Transversal asymmetry described 19.74% of all variability and corresponded to components PC2, PC8 and PC10. Together, PC2 described 14.95% of the variability of all subspaces. One spine within the transversal segment was slightly shorter than the other, but they both pointed in the same direction. The core of the coenobium was rotated upwards on the right side, therefore the cells were slightly misaligned. PC8 described 2.54% of total variability. The entire coenobium was spirally twisted. The spines were thus deflected, but were otherwise the same in length. The spiraling also deformed the cells. PC10 corresponds to 1.29% of the variability. Coenobium twisted spirally but much less than in PC8. The spines were the same length but slightly skewed. Similarly, the coenobium cells were slightly misaligned. For all components, the coenobia were upwardly directed on the right side.

3.3.4 Strain D

The consensual coenobium from strain D was deflected upwards on the right side. Spines emerged transversally from the coenobium core. The cells of the coenobium were all the same size.

Symmetric variation described a total of 76.44% of the variability and was represented by the components PC1, PC4 and PC9. PC1, which accounted for 63.95% of the variability, described both spine and core deformations (see Fig. 23). On one margin of the spectrum, the spines were strongly directed towards each other and then at the other end they were almost vertically extending away from the coenobium core. The coenobium core was then very wide and stretched on one margin of the morphospace spectrum. On the other margin, the core was strongly constricted into itself. The PC4 component accounted for 6.19% of total variability. This time it was mainly deformation of the coenobium core. On one margin of the morphospace spectrum the cells were shrunken and then significantly enlarged on the other margin. The PC9 component together described 1.20% of the variability and again described mainly the shape changes of the coenobium core. It shrunk significantly on one margin and the cells were taller than wide. On the other margin of the morphospace spectrum, the cells became significantly wider. All of the named components had the coenobium slightly skewed up on the right side.

Horisontal asymmetry accounted for 6.36% of total variability and described components PC3 and PC8. PC3 explained 6.99% of the variability of all subspaces. This component corresponded to spine deformations. One spine from the horisontal segment was much shorter and extended horisontally from the coenobium core. The other spine then curved transversally outwards. PC8 described 2.25% of total variability. The spines were slightly deformed especially in terms of their

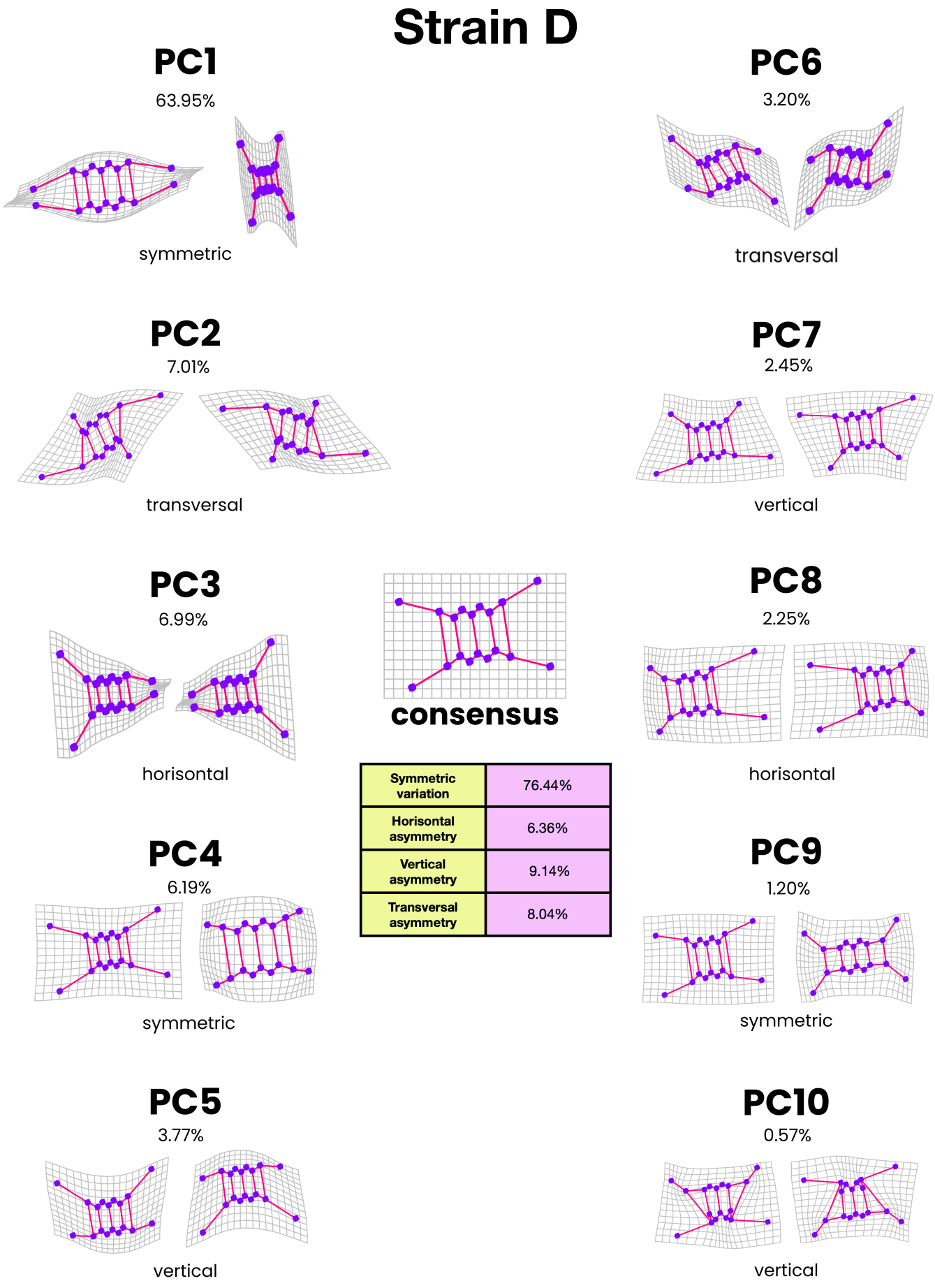

Figure 23. ***Strain D:*** *A scheme showing Desmodesmus communis coenobia reconstructed by principal component analysis of biradial symmetry. The first ten principal components are illustrated. These configurations represent the most peripheral positions that the shapes assume in morphospace. The configuration of the consensus coenobium is illustrated in the middle. A table showing the relative amounts of symmetry variation and the three types of asymmetry are also shown.*

length. One spine was always significantly longer than the other. The coenobium core was deformed especially in the area where the longer spines were emerging from. This marginal cell was much smaller than the rest of the cells. For both components PC3 and PC8, the coenobia were upwardly directed on the right side.

Vertical asymmetry accounted for 9.14% of all variability and described components PC5, PC7 and PC10. PC5 expressed 3.77% of total variability and mainly described the deformation of the spines. One spine from the vertical segment was much shorter than the other. Both then bent in the same direction, but the longer spine was more skewed. The PC7 component described a total variability of 2.45%. These were again mainly changes in spine shape, which differed especially in length. The longer spine within the vertical segment pointed in a similar direction as the spines of the consensual coenobium, while the shorter spine was slightly more outwardly deflected. The PC10 component then accounted for 0.75% of all variability. This component described an extreme asymmetry of the coenobia core and spines. The marginal cells were highly deformed on one side, where they almost intersected with the neighbouring cells. This caused deformation of the longer spines as the landmarks from which they emerged were out of their normal position. The shorter spines then appeared relatively symmetric but were more skewed outwards compared to the consensus. All of the mentioned components had the coenobium slightly skewed up on the right side.

Transversal asymmetry corresponded to 8.04% and was represented by components PC2 and PC6. The PC2 component then expressed 7.01% of the variability. Extreme asymmetry of both spines and coenobium core could be observed on this component. The entire coenobium twisted spirally, which maximally deflected the coenobium cells. The marginal cells were the most asymmetric and partially overlapped the landmarks of the neighbour cells on one side, causing a triangular shape of the marginal cells. The spine, emerging from the region of overlapping landmarks, was then always significantly shorter and more deflected. PC6 accounted for 3.20% of the variability among all subspaces. This was a similar deformation to that observed in the PC2 component. However, it was slightly less pronounced and the longer spine emerged from the overlapping landmarks this time. For all components, the coenobia were upwardly skewed on the right side.

4. Discussion

4.1 Coenobial asymmetry as a consequence of different conditions occurring under planktonic life history

Phenotypic plasticity of *Desmodesmus communis* in response to changes in environmental conditions has been described in the past mainly as a difference between single-cell and multicellular morphotypes or spiny to spineless morphotypes (Shubert *et al.*, 2014). For this reason, I focused my work on a different kind of phenotypic plasticity, namely asymmetry of the coenobial shape. The influence of different environmental conditions such as *p*H, predation pressure or the presence of heavy metals has also been studied (Hessen & Van Donk, 1993; Peña-Castro *et al.*, 2004; Yang *et al*., 2016). However, no study has been conducted on phenotypic plasticity (asymmetry) of *Desmodesmus communis* as a consequence of planktonic life history.

The ability to stay in the euphotic zone is vital for algae as photosynthetic organisms, and *Desmodesmus* is no exception (Masojídek *et al.*, 2013). As found in the study by Padisák *et al.* (2003) the symmetry of algal thallus plays a key role in persisting in the euphotic zone. Although *Desmodesmus communis* has been found to voluntarily relinquish its position in the euphotic zone at some stages in its life cycle by forming eight to sixteen-celled coenobia and sinking to deeper levels of the water column, this is primarily a mean of escape from predators (Lürling, 2003). What plays a role in staying in the euphotic zone for the typical four-celled coenobia of *Desmodesmus communis* has not been studied. In my thesis, I hypothesized that the ability to form symmetric phenotypes could be the explanation. The question remained, however, which conditions possibly occurring in plankton would result in a higher asymmetry of coenobial shapes.

In my thesis I simulated three different scenarios that can occur living a planktonic life (Holgerson *et al.*, 2022). A mixed, stationary and stationary-mixed state was induced in order to observe how such water conditions affected the symmetry of *Desmodesmus*. In my thesis, I focused on coenobia because they are the primary state most commonly found in the euphotic zone as opposed to single-cell and eight to sixteen-celled coenobia, which are formed only under certain induced conditions (cyclomorphosis, predatory pressure etc.). I expected that mixing would result in more precise symmetry of four-celled coenobia, as they are constantly subjected to mixing and so their thalli would be forced to adapt to such pressure. It was also important to take into account the fact that *Desmodesmus* is a true planktonic organism and thus it was expected that their thalli would develop symmetrically in their natural turbulent environment (Hegewald & Braband, 2017). On the other hand, I assumed that the descending four-celled coenobia would grow more asymmetric, which would further encourage sinking. Indeed, it was possible that coenobia living in unmixed environments simply grew asymmetrically because such a lifestyle is not necessarily natural to them.

The first part of the investigation involved an asymmetry analysis involving both coenobium core and spines. In nature, spines represent a critically important component of the coenobium. They are important elements of the thallus that exhibit antipredatory effects, which has been suggested in several studies. The spines could act as a mechanical defense, but at the same time they might increase the surface area of the coenobium and thus deter smaller predators from ingesting it (Lürling, 2003). However, this explanation is not entirely convincing, as no association between the presence of kairomones and the phenotypic plasticity of the spines has been proven to date. So I suggested another possible role that the spines could be playing and that was to assist in maintaining *Desmodesmus* coenobia in the euphotic zone.

Live variation in shape of the spines was noticed during light microscopic observations. However, these shape changes occurred only during extreme water movement on the slide, which bent or broke the spines. In calmer conditions, the spines did not bend or otherwise change shape. I therefore presumed that the shape of the spines was already pre-determined during ontogeny. Nevertheless, I expected the spines to have the greatest influence on the resulting degree of asymmetry. They are the peripheral regions most exposed to environmental challenges, and in addition, they happen to be much thinner polysaccharide structures compared to the coenobium core and thus probably more susceptible to morphological changes (Baudelet *et al.*, 2017). However, the question remained whether the spines were phenotypically plastic or flexible. If this were phenotypic flexibility, it would mean that the spines are able to change shape during the life cycle in a reversible manner partly independent of their foundation in ontogeny.

The analysis including spines demonstrated that most asymmetric coenobia occurred under the stationary-mixed treatment. The stationary-mixed treatment was intended to simulate the conditions of water bodies that are mixed only intermittently for short periods of time (Holgerson *et al.*, 2022). If *Desmodesmus* responded in nature as it did in these simulated conditions, this would mean that we should observe more asymmetric coenobia of *Desmodesmus communis* in such partially mixed natural environments. Under such conditions, it would probably be futile for *Desmodesmus communis* to put energy into the formation of a symmetric coenobium. Each of the changing conditions requires a different coenobial shape and changing it for short periods of time would thus be very challenging. To confirm this hypothesis, an analysis of natural samples from such partially mixed waters should be performed in the future, to compare *in situ* and *in vitro* responses.

Another explanation, however, may be that the stationary-mixed treatment was simply not able to properly match the conditions in nature. Thus, for *Desmodesmus*, the treatment may have represented extremely unnatural, unknown conditions for which it lacked any adapted response. The uncertain pattern of mixing and non-mixing may have made the conditions so unpredictable for *Desmodesmus* that it was unable to functionally react to them. This was manifested by the chaotic growth of asymmetric spines.

Relatively high levels of asymmetry also occurred under the mixed treatment, which was a surprising result given the initial hypothesis. The mixed environment, which should be natural for *Desmodesmus,* caused its spines to grow relatively asymmetrically. It is therefore possible that the initial state of coenobial shape is not symmetric but asymmetric. In fact, in a turbulent environment,

Desmodesmus does not need to actively try to balance the shape of its coenobia, since it is not at risk of sinking anyway.

The lowest level of asymmetry was observed in coenobia that underwent the stationary treatment. The initial hypothesis expecting a high degree of asymmetry arising from this treatment was therefore disproven. This finding reflects the results of the study by Padisák *et al.* (2003), who reported that the more symmetric an organism is, the slower it sinks down in the water column. When the stable position of coenobia in the euphotic zone is not aided by water mixing, it is critically important for them to find another way to sink at least as slowly as possible. This is achieved by the formation of highly symmetric coenobia and spines. Any deflection of the spines out of symmetry means a tilting of the coenobium and thus a much faster sinking (Padisák *et al.*, 2003)

As already mentioned, before starting the analysis I had already assumed that the spines would introduce the most asymmetry into the shape of coenobia. This was confirmed in the second part of the analysis No. 1. In this section, the effect of spines was eliminated from the analysis and only changes in the shape of the coenobium core were observed. Surprisingly, the treatment that gave rise to the greatest overall asymmetry differed from the analysis involving spines. This time the highest level of asymmetry resulted from the mixed treatment. This means that although extreme asymmetry of spines was produced under the stationary-mixed treatment, asymmetry of both spines and coenobia cores resulted from the mixed treatment. This would seem to confirm the complete disregard for symmetry of *Desmodesmus* living in permanently mixed environments. Not only it would be unnecessary to put energy into the formation of symmetric spines, it would also be redundant to expend it on a symmetric core.

The explanation for why only the spines were asymmetric under the stationary-mixed treatment may be the aforementioned unpredictability of the conditions in this environment. The deformities I observed on coenobia under this treatment could have been due to phenotypic flexibility that applied only to the spines. Thus, this would mean that the spines are able to change shape during short-term changes in conditions, but the core remains the same. It is possible, therefore, that the coenobia I captured during photography could have been the ones originating during the mixing phase. During the stationary phase, the coenobia may have been symmetrized using spines to prevent short-term sinking pressure effects

Under stationary treatment, the cores of coenobia were found to form rather asymmetrically, unlike the spines under the same treatment. This could be due to the fact that it is the spines that play the biggest role in preventing sinking. The shape of the coenobium core simply doesn't affect sinking as much as the spines. Moreover, the asymmetry of the coenobia cores is often represented by a deflection to a certain side, which I assume is again compensated by the symmetry of spines.

Overall, it should be added that the analysis excluding spines showed a much lower level of asymmetry than when spines were included. The intervals started at smaller units and spanned over much narrower ranges. This therefore confirmed my hypothesis that it is the spines that caused such high levels of coenobial asymmetry in the first part of the analysis.

The second aspect I observed in my analyses was on which symmetry axis the most asymmetry occurs. Whether the analysis was with or without spines, the axis that was clearly the most asymmetric was the transversal axis. This was again a very interesting finding, because studies that

have looked at asymmetry in other algal species in the past, for example diatoms, discovered that the asymmetry most often occurs on the horisontal axis (Woodard, 2023). In desmids, on the other hand, the highest asymmetry observed was usually with regards to the vertical axis (Neustupa, 2013). Unfortunately, there are no studies that address the asymmetry in this entire lineage, so one can only speculate as to why *Desmodesmus* differs so much. The transversal asymmetry could represent a lineage specific feature, which could be a very interesting breakthrough in the morphological studies of these organisms. This phenomenon could represent a completely innovative view of physiological integration and how the cells within the coenobium communicate with each other. In diatoms and desmids, asymmetry has become an enticing subject of study, as it is now clear that it has a major impact on their survival. The same should therefore be done with *Desmodesmus* and consequently with the other genera belonging to Scenedesmaceae.

The other asymmetry axes then behaved rather inconsistently. Both horisontal and vertical axis showed some degree of asymmetry, but these were erratic results in which it was difficult to find a pattern. Personally, I believe that since asymmetry is inherent in nature, it is only natural that the other axes also showed some degree of it. Compared to the rest, the degree of transversal asymmetry was so significant that I consider it an unusual phenomenon found in my thesis. However, I consider the asymmetry of the horisontal and vertical axis to be a natural consequence of being a living non-perfect organism.

It is also very relevant to mention that strain A was the only one that differed significantly from the other strains. In the analysis involving spines, the mixed treatment resulted in the highest asymmetry. For the other strains, the mixed treatment was rather secondary, although still relatively high. More interestingly, the other treatments reached relatively low values and ranged within very narrow intervals. Coenobia in the other treatments were therefore extremely symmetric. However, the most significant difference was that the lowest observed asymmetry was located on the transversal axis. When looking at strain A without spines, we could observe variations from the other strains as well. The transversal axis did indeed achieve the highest asymmetry this time, but very high asymmetry was also achieved in the stationary treatment, which was very odd compared to the other strains with and without spines. A possible explanation for this unpredictable behavior may be that strain A has been growing in the collection for approximately fifty years. In my opinion, this could be a long enough time for such a culture to lose the phenotypic plasticity typical for *Desmodesmus* living in nature. A strain that has been exposed only to a stationary environment for fifty years is likely to be highly adapted to it. The phenotype favored in a stationary environment will then be strongly selected for, and under other induced conditions the strain will react chaotically and unpredictably (Scheiner & Levis, 2021). In order to re-establish the typical plasticity responding functionally to different natural conditions that *Desmodesmus* exhibits in nature, it would be needed to subject this strain to mixing experiments over a longer period of time, thus allowing for multiple generations to be alternated.

4.2 The relationship between the size of the coenobium and its asymmetry

The aim of this analysis was to determine what the relationship is between the observed asymmetry and the size of the individual coenobia. Fairly pronounced size differences were observed between and within strains, so I was interested to see if there would also be differences in shape.

Desmodesmus communis coenobia gets larger with age, which is different from diatoms, for example, which get smaller the older they get (Hense & Beckman, 2015; Kulichová & Urbánková, 2020).

Generally in nature, older individuals become deformed and less symmetric. This can be demonstrated in a species very phylogenetically distant from *Desmodesmus*, the human species. Studies have shown that the human face becomes less symmetric with age (Linden *et al.*, 2018). The same has been observed in certain plants as well (Téllez & Møller, 2006). This is hardly surprising, since environmental stressors have a detrimental effect on living bodies, which gradually decay with age. Hence, I expected a similar positive correlation pattern for *Desmodesmus*.

When observing the sizes of coenobia from each strain, I discovered that the largest coenobia have grown in strains C and D under the mixed treatment. The coenobia sizes in these strains and treatment were extremely deviated from the rest. This could theoretically indicate that the pond and lake environment during the mixed periods simply gave rise to larger individuals. Even the heaviest individual will not sink in a mixed environment. In the stationary treatment, the smaller size of coenobia makes sense again because smaller and therefore lighter coenobia will not sink as quickly. To confirm this hypothesis, additional repetitions of the experiment would be required. Interestingly, no significant differences in size was observed between treatments in strain B, which was collected from the river. The river is inherently a consistently mixed body of water. *Desmodesmus communis* naturally living in such an environment is not adapted to stationary environmental conditions and so was unable to respond to them in such a short time. A prolonged repetition of the experiment would again be needed to confirm the hypothesis.

The fact that interested me the most was whether larger individuals become more asymmetric as is the case with other living organisms. As mentioned above, I expected this to be the case. However, an analysis of the relationship between asymmetry and size (and in this case age) of *Desmodesmus* coenobia yielded rather unexpected results.

A negative correlation between the variables was observed for all treatments in strains B and D. The same was true for strain C, but the correlations were not as significant. The negative correlation meant that the smaller the coenobia were, the higher their asymmetry was. Thus, the older individuals were more symmetric in these strains, which presents a complete contradiction to how other living organisms age.

Desmodesmus communis in cultivation usually reproduces asexually by means of the parent sporangium, which breaks open and gives rise to four new small coenobia (Komárek & Fott, 1983). Therefore, the asymmetry I observed in small individuals could be the result of deposition in the maternal coenobium. The small coenobia are tightly squashed in the sporangium and their shape after

their emergence reflects their residence in the sporangium. And during their lifetime, the coenobia gradually become straightened, and I assume this is mainly in the area of the spines, which appeared to be the most asymmetric during the analysis. This would further confirm my discovery made in the first analysis that the spines are phenotypically flexible and change shape during life.

It is also highly fascinating that the most significant negative correlation was observed for strains B and D, specifically under the stationary-mixed treatment. Here, the small coenobia were the most asymmetric of all. This is interesting in light of the first analysis, which revealed a high degree of asymmetry when subjected to this particular treatment. This may reflect my hypothesis that with the uncertainty that comes with occasional mixing and occasional resting it is impossible for *Desmodesmus* to predict the future state and so it is very challenging for small coenobia to straighten the spines.

Strain A behaved inconsistently in analysis again. In some treatments, the small coenobia were slightly more symmetric than the large ones, and in others it copied the same behavior as the other strains showed. I again attribute this to the age of the whole strain and its inability to be plastic under unknown natural conditions.

The findings of this analysis are very intriguing indeed. It is a phenomenon that could open the door to further similar studies, as it is possible that the same behavior will be shown in other algae that reproduce in this way. But it is also plausible that this is again a very specific pattern of life for this algal lineage.

4.3 Symmetric and asymmetric variability of individual strains

Analysis No. 3 was designed to further illustrate the degree of symmetric and asymmetric variation within individual strains of *Desmodesmus communis*. Such analyses have been done on other distant algal species in the past such as the diatom *Frustulia* or the green macroscopic algae *Halimeda tuna* (Kulichová & Urbánková, 2020; Neustupa & Němcová, 2018). These analyses provided a deeper understanding of the mechanisms of phenotypic plasticity of the organisms in question. All body parts into which an organism can be divided should be genetically identical to each other which should potentially result in an ideal symmetry. Although some objects in nature may seem perfectly symmetric, this is usually not the case and therefore it is clear that fluctuations in symmetry are more likely to be caused by environmental stressors or developmental instability (Gerber & Savriama, 2021; Kulichová & Urbánková, 2020). And as has been found, it is the shape plasticity that often enables algae to withstand such stress conditions. The study of the very intricate algal shapes is therefore a very useful way to understand their ecology and developmental processes (Klingenberg, 2019).

In my previous analyses I found a high degree of asymmetry on the transversal axis. In this analysis, I then wanted to hopefully confirm this finding. This time, however, I analyzed the strains without the signal introduced by the different treatments.

My thesis has shown that symmetric variation among coenobia in all four strains of *Desmodesmus communis* is the most pronounced component of shape variation. That is, differences

between individual coenobia within a strain were more prominent than asymmetry within the coenobial segments. In the largest proportion, symmetric variation was manifested as spine plasticity. In all strains, the spines often either diverged transversally from each other or intersected, alternatively. To a lesser extent, however, symmetric variation was also manifested as deformations in the shape of coenobial cores. This was mostly represented by a change in the proportion of coenobium height and width. The largest contribution to the symmetric variation was always manifested on the first principal component (PC1) in all the strains. A study on the diatom genus *Frustulia* described the same phenomenon as my thesis (Kulichová & Urbánková, 2020). The shape differences between cells within one strain were more pronounced than the differences within the asymmetric segments of the cells themselves. In contrast, in several species of the genus *Micrasterias*, such a large difference between symmetric variation and asymmetric components (specifically the vertical asymmetry) was not observed. The PC1 component described vertical asymmetry in two of the three species. Symmetric variation then corresponded to the PC1 component in only one species. The total values of symmetric variation and vertical asymmetry were both similarly high in all species. Thus, the degree of asymmetry between individuals was comparable to the degree of asymmetry within individuals in this study (Neustupa, 2013). In my thesis, on the other hand, the gap I observed between the value of the first principal component (expressing symmetric variability) and the second principal component (expressing various asymmetry types) was indeed considerably large.

Interestingly, although all the strains differed significantly in the other asymmetric components, they matched in one respect. The second principal component (PC2) described the transversal asymmetry in all strains except strain A. Thus, in these three strains, the relationship between the transversal segments of the coenobium was most significant for the resulting shape of all individuals. The transversal asymmetry in all strains studied manifested itself mainly as a spiral rotation that curved the spines and more or less deflected the coenobium cells from their typical location. This is an additional evidence that under certain environmental conditions *Desmodesmus communis* generally reacts by plasticity on the transversal segment of asymmetry. For comparison, in a similar study of the diatom genus *Navicula*, it was shown that all symmetric and asymmetric components (including transversal) reached very similarly high values (Woodard *et al.*, 2016). Such a determining proportion of transversal asymmetry, therefore, has not been observed in other algae. For example, in a study of symmetric and asymmetric variation in the green algae *Micrasterias*, transversal asymmetry came out considerably less significant than the rest of the components in all samples studied. Similarly, when studying the different species of the genus *Frustulia*, transversal asymmetry appeared rather negligible, as its manifestation was shown only at PC6 and at a very low percentage.

Since such a high proportion of transversal asymmetry is apparently not very common in algae, it would be very interesting to look into this aspect in the future and possibly describe the communication processes between the cells during ontogenesis. Since *Desmodesmus* is generally formed by more than one cell, the transversal asymmetry could originate from a certain lack of cooperation between individual cells within the coenobium during ontogenesis. As I noticed in my previous analyses, *Desmodesmus communis* is capable of phenotypic flexibility (especially in the spine region) and that could possibly also play a key role. Diatoms, for example, are inherently very

rigid in shape, due to their silicate frustules. Their shape is therefore determined in their development. For *Desmodesmus*, however, this is not the case. The shape of the spines is responsible for the highest asymmetry of the entire coenobium. Small coenobia have spines that are extremely asymmetric and straighten out during their life cycle. It is possible that the communication between the spines from opposite ends of the coenobium, and especially those transversely opposite, is significantly more intricate than for spines originating from the same marginal cell. This mismatch in a phenotypic response may be responsible for the high transversal asymmetry found here.

The difference between the most determining asymmetric components in *Desmodesmus* and the other algae mentioned could therefore be their completely different body compositions. Diatoms generally consist of only one cell composed of two valves. Thallus of *Micrasterias* is principally composed of two semicells. Both diatoms and desmids exhibit allometry during their life cycle Allometry describes the relationship between size and shape of an object (Dujardin, 2017). Because of that *Micrasterias* has always shown increased vertical (up-down) asymmetry in most studies, based on the temporally separated growth of the two semicells. Thus, different environmental conditions can affect each semicell during its life cycle. In a study of the pennate diatom species *Luticula*, the highest asymmetry observed was horisontal (left-right) which resulted from temporally separated successive silicification on the right and left side of an individual. Vertical asymmetry in *Luticula* has been shown to be very low, since one part of the valve always forms according to the other, hence their high similarity (Kulichová *et al.*, 2019; Woodard *et al.*, 2016). Although the same high degree of left-right asymmetry was expected in the genus *Navicula*, it was not observed here (Woodard *et al.*, 2016).

In addition to transversal asymmetry, vertical asymmetry then also appeared to determine the shape of the coenobia in all strains. While the latter described even the most variability of all the asymmetric components overall for strains A, B, and D, its influence was often reflected in only small percentages on the less determinate principal components. In addition, even visualizations of the components with respect to vertical asymmetry showed much higher symmetric morphology than, for example, most components describing the transversal and horisontal asymmetry. This would show that the vertical segment, although very important for the shape, produces a relatively high symmetry. This would confirm my hypothesis that spines that grow from the same side are more similar to each other, since the same single cell is responsible for their development. Although the horisontal asymmetry components in strains A, B and D reached the smallest proportion of the total variability, it was expressed on more shape-determining components much more frequently than vertical asymmetry. Extreme horisontal asymmetry was also much more evident on the morphospace visualization. Thus, this confirms that not only transversely distant spines but also spines horisontally growing out of different marginal cells appear highly asymmetric due to the inability of communication between the cells.

As already mentioned, the strains differed quite a lot in the distribution of symmetric and asymmetric variability. This could reflect their distinct genetic basis. Strain A differed the most from the other strains in the symmetric and asymmetric components. Strain A was the only strain with the PC2 describing the horisontal and not the transversal asymmetry. This was interesting, but not striking, as previous analyses had also shown this type of asymmetry to be very defining for strain A. The vertical segment also accounted for a very high share of the total asymmetry, which also mirrored the

results of the previous analyses. This was not the case for transversal asymmetry, which turned out to be relatively insignificant for strain A again. Transversal asymmetry was described at only very low percentages on the components PC6, PC9 and PC10. Even visualization of these transversal components did not show a large degree of this type of asymmetry. This was not particularly strange, as in previous analyses this strain had already behaved unpredictably and chaotically compared to the other strains. Since this is a strain that has been in the collection for about fifty years, a high genetic divergence from the other strains I have isolated from the wild is to be expected.

In terms of similarity between strains, the river strain B and the lake strain D were most similar in symmetric and asymmetric variation to each other. They were highly similar in the first four principal components. Their values were almost identical, and likewise, after visualization, it was clear that the components expressed a very similar type of symmetry and asymmetry. For these two strains, the highest symmetric variation was observed. Thus, the differences between coenobia (versus differences within coenobia) were much higher here compared to strains A and C. Nonetheless, the visualization of strain D showed the most extreme deformations across all components. In this strain, the increased level of asymmetry could have been genetically fixed. A specific asymmetric phenotype that might have originated due to certain environmental conditions in the past may have become genetically assimilated due to the process of selection on that specific asymmetric phenotype (Waddington, 1961). A very high asymmetry, which seemingly did not originate from present environmental stress, was also observed in the diatom *Frustulia*, for example. Some species of this alga have been shown to have a high levels of inherited asymmetry, that seemed to be passing on further to subsequent generations (Kulichová & Urbánková, 2020).

For future studies, it would be essential to focus more on the relationship between the segments of asymmetry within a single coenobium and their communication in the process of developmental plasticity and phenotypic flexibility. Indeed, it is still not entirely clear what communication pathways the cells share with each other. What is the role of the middle cells? How complex is the transfer of information from one margin to the other? Could the various planktonic conditions be the source of the miscommunication? All this remains a question for my further research.

5. Conclusions

In my thesis, I observed the phenotypic plasticity of *Desmodesmus communis* as a result of various environmental factors associated with the planktonic life history. I tried to mimic such conditions and observed how the symmetry of coenobia changed.

In all analyses, a pattern was observed that showed a relationship between the asymmetry of *Desmodesmus communis* coenobia and planktonic life history. This relationship was most prominent in the spines region, in which a relatively high degree of flexibility was observed. The spines are able to morphologically adapt to changes in environmental conditions and thus have the greatest influence on the final shape of the entire coenobium. But it is also the spines that are responsible for the high asymmetry of the small coenobia that have just emerged from the mother coenobium. Large adult coenobia then become more symmetric over time. This was a very interesting discovery in the context of the study of aging, as it is a completely opposite behavior to other living organisms.

The most surprising finding was the fact that this algae responds to environmental changes by immense plasticity in the transversal segment of asymmetry, which has not yet been observed in other algae. This is a breakthrough that could open up entirely new possibilities for morphometric studies of these algae, and thus discovering more about its life history.

It was also confirmed that coenobia living in a constitutively mixed aquatic environments do not need to invest energy in symmetric cores and spines, and thus develop overall highly asymmetric morphology. Conversely, in stationary environments, it turned out to be extremely important for coenobia to grow symmetrically so that they do not sink as quickly in the water column. If *Desmodesmus communis* inhabits an environment where periods of mixing and resting alternate, coenobia cores have been observed to emerge highly symmetric and changes in the shape of *Desmodesmus communis* were then concentrated on the spine regions. This again reflects the fact that *Desmodesmus* is able to allocate energy where it is needed. With fluctuating environmental conditions, it would not be meaningful to repeatedly change the shape of both spines and cores. Shape changes are therefore concentrated on the spines here, which during the short non-mixed periods balance the entire symmetry of the coenobium.

For future experiments, it would be certainly necessary to compare the behavior of natural populations and populations from my cultures. Experiments would also need to be carried out over longer periods of time to allow for manifestation of other aspects of plasticity. In other respects, I think my results are certainly intriguing and fruitful for future research on *Desmodesmus communis* and, by extension, other algae morphologically related to it.

6. References

Adams, D. C., Rohlf, F. J., & Slice, D. E. (2004). Geometric morphometrics: Ten years of progress following the “revolution.” Italian Journal of Zoology, 71(1), 5–16. doi:10.1080/11250000409356545

Adams, D. C., Rohlf, F. J., & Slice, D. E. (2013). A field comes of age: Geometric morphometrics in the 21st century. Hystrix, 24(1). doi:10.4404/hystrix-24.1-6283

Alberghina, J. S., Vigna, M. S., & Confalonieri, V. A. (2006). Phylogenetic position of the Oedogoniales within the green algae (Chlorophyta) and the evolution of the absolute orientation of the flagellar apparatus. Plant Systematics and Evolution, 261(1–4), 151–163. doi:10.1007/s00606-006-0449-2

Andersen, R. A. (2005). Algal culturing techniques. Elsevier Academic Press, New York, 578 p.

Bakuei, N., Amini, G., Najafpour, G., Jahanshahi, M., & Mohammadi, M. (2015). Optimal cultivation of *Scenedesmus* sp. microalgae in a bubble column photobioreactor. Indian Journal of Chemical Technology, 22, 20–25.

Baudelet, P.-H., Ricochon, G., Linder, M., & Muniglia, L. (2017). A new insight into cell walls of Chlorophyta. Algal Research, 25, 333–371. doi:10.1016/j.algal.2017.04.008

Baverstock, K. (2021). The gene: An appraisal. Progress in Biophysics and Molecular Biology, 164, 46–62. doi:10.1016/j.pbiomolbio.2021.04.005

Benítez, H. A., Lemic, D., Villalobos-Leiva, A., Bažok, R., Órdenes-Claveria, R., Pajač Živković, I., & Mikac, K. M. (2020). Breaking symmetry: Fluctuating asymmetry and geometric morphometrics as tools for evaluating developmental Instability under diverse agroecosystems. Symmetry, 12(11), 1789. doi:10.3390/sym12111789

Caillon, F., Bonhomme, V., Möllmann, C., & Frelat, R. (2018). A morphometric dive into fish diversity. Ecosphere, 9(5), doi:10.1002/ecs2.2220

Černá, K., & Neustupa, J. (2009). The pH-related morphological variations of two acidophilic species of Desmidiales (Viridiplantae) isolated from a lowland peat bog, Czech Republic. Aquatic Ecology, 44(2), 409–419. doi:10.1007/s10452-009-9296-x

Dehning, I., & Tilzer, M. M. (1989). Survival of *Scenedesmus acuminatus* (Chlorophyceae) in darkness. Journal of Phycology, 25(3), 509–515. doi:10.1111/j.1529-8817.1989.tb00256.x

Dujardin, J.-P. (2017). Modern morphometrics of medically important arthropods. Genetics and Evolution of Infectious Diseases, 285–311. doi:10.1016/b978-0-12-799942-5.00013-5

Duncan, E. J., Gluckman, P. D., & Dearden, P. K. (2014). Epigenetics, plasticity, and evolution: How do we link epigenetic change to phenotype? Journal of Experimental Zoology Part B: Molecular and Developmental Evolution, 322(4), 208–220. doi:10.1002/jez.b.22571

Fučíková, K., Lewis, P. O., Neupane, S., Karol, K. G., & Lewis, L. A. (2019). Order, please! Uncertainty in the ordinal-level classification of Chlorophyceae. PeerJ, 7, e6899. doi:10.7717/peerj.6899

Garland, T. (2011). The Flexible Phenotype: A body-centred integration of ecology, physiology, and behaviour. Animal Behaviour, 82(3), 609–610. doi:82. 609-610. 10.1016/j.anbehav.2011.06.012

Gaysina, L. (2024). Influence of pH on the morphology and cell volume of microscopic Algae, widely distributed in terrestrial ecosystems. Plants, 13, 357. doi:10.3390/plants13030357

Gerber, S., & Savriama, Y. (2021). Symmetry of shapes in biology: from D'Arcy Thompson to morphometrics. doi:10.1002/9781119476870.ch1

Guiry, M. D., & Guiry, G. M. (2024). AlgaeBase. World-wide electronic publication, University of Galway. https://www.algaebase.org; searched on July 14, 2024.

Hammer, D. A. T., Ryan, P. D., Hammer, Ø., & Harper, D. A. T. (2001). Past: Paleontological statistics software package for education and data analysis. Palaeontologia Electronica, 4(1). http://palaeo-electronica.org/2001_1/past/issue1_01.htm

Hazra, A. (2017). Using the confidence interval confidently. Journal of Thoracic Disease, 9(10), 4124–4129. doi:10.21037/jtd.2017.09.14

Hegewald, E., & Braband, A. (2017). A taxonomic revision of *Desmodesmus* serie *Desmodesmus* (Sphaeropleales, Scenedesmaceae). Fottea, 17, 191–208. doi:10.5507/fot.2017.001

Hense, I., & Beckmann, A. (2015). A theoretical investigation of the diatom cell size reduction–restitution cycle. Ecological Modelling, 317, 66–82. doi:10.1016/j.ecolmodel.2015.09.003

Hessen, D., & Donk, E. (1993). Morphological changes in *Scenedesmus* induced by substances released from *Daphnia*. Archiv für Hydrobiologie, 127(1), 129–140. doi:10.1127/archiv-hydrobiol/127/1993/129

Holgerson, M., Richardson, D., Roith, J., Bortolotti, L., Finlay, K., Hornbach, D., Gurung, K., Ness, A., Andersen, M., Bansal, S., Finlay, J., Cianci-Gaskill, J., Hahn, S., Janke, B., McDonald, C., Mesman, J., North, R., Roberts, C., Sweetman, J., & Webb, J. (2022). Classifying mixing regimes in ponds and shallow lakes. Water Resources Research, 58. doi:10.1029/2022WR032522
Johannsen, W. (1911). The genotype conception of heredity. The American Naturalist, 45(531), 129–159. doi:10.1086/279202

Klingenberg, C. P. (2019). Phenotypic plasticity, developmental instability, and robustness: The concepts and how they are connected. Frontiers in Ecology and Evolution, 7. doi:10.3389/fevo.2019.00056

Komárek, J., & Fott, B. (1983). Chlorophyceae (Grünalgen), Ordnung Chlorococcales. Nordic Journal of Botany, 5(1), 111–111. doi:10.1111/j.1756-1051.1985.tb02080.x

Kost, C. (2008). Chemical communication. Encyclopedia of Ecology, 557–575. doi:10.1016/b978-008045405-4.00036-7

Krienitz, L. (2009). Algae. Encyclopedia of Inland Waters, 103–113. doi:10.1016/b978-012370626-3.00132-0

Kulichová, J., & Urbánková, P. (2020). Symmetric and asymmetric components of shape variation in the diatom genus *Frustulia* (Bacillariophyta). Symmetry, 12, 1626. doi:10.3390/sym12101626

Kulichová, J., Neustupa, J., Vrbová, K., Levkov, Z., & Kopalová, K. (2019). Asymmetry in *Luticola* species. Diatom Research, 34(2), 67–74. doi:10.1080/0269249X.2019.1604435

Levin, M. (2001). Asymmetry of body and brain: Embryological and twin studies. International Encyclopedia of the Social & Behavioral Sciences, 853–859. doi:10.1016/b0-08-043076-7/03356-8

Linden, O. E., He, J. K., Morrison, C. S., Sullivan, S. R., & Taylor, H. O. B. (2018). The relationship between age and facial asymmetry. Plastic and Reconstructive Surgery, 142(5), 1145–1152. doi:10.1097/PRS.0000000000004831

Lürling, M. (2003). Phenotypic plasticity in the green algae *Desmodesmus* and *Scenedesmus* with special reference to the induction of defensive morphology. Annales de Limnologie - International Journal of Limnology, 39(2), 85–101. doi:10.1051/limn/2003014

Lürling, M., & Van Donk, E. (2000). Grazer-induced colony formation in *Scenedesmus*: are there costs to being colonial? Oikos, 88(1), 111–118. doi:10.1034/j.1600-0706.2000.880113.x

Martindale, M. Q., & Henry, J. Q. (1998). The Development of radial and biradial Symmetry: The evolution of bilaterality. American Zoologist, 38(4), 672–684. doi:10.1093/icb/38.4.672

Masojídek, J., Torzillo, G., & Koblížek, M. (2013). Photosynthesis in microalgae. Handbook of Microalgal Culture, 21–36. doi:10.1002/9781118567166.ch2

McKenna, K. Z., Gawne, R., & Nijhout, H. F. (2022). The genetic control paradigm in biology: What we say, and what we are entitled to mean. Progress in Biophysics and Molecular Biology, 169–170, 89–93. doi:10.1016/j.pbiomolbio.2022.02.003

Giennap, P., Merilä, J. (2017): Evolutionary responses to climate change. doi:10.1016/b978-0-12-409548-9.10263-5

Morales, E., & Trainor, F. (2022). Algal phenotypic plasticity: Its importance in developing new concepts: The case for *Scenedesmus*. ALGAE, 12, 147–157.

Nettleton, D. (2014). Selection of variables and factor derivation. Commercial Data Mining, 79–104. doi:10.1016/b978-0-12-416602-8.00006-6

Neustupa, J. (2013). Patterns of symmetric and asymmetric morphological variation in unicellular green microalgae of the genus *Micrasterias* (Desmidiales, Viridiplantae). Fottea, 13, 53–63. doi:10.5507/fot.2013.005

Neustupa, J. (2015). Chlorophyta (excl. Ulvophyceae). In W. Frey (Ed.), Syllabus of plant families, Part 2/1, Photoautotrophic eukaryotic algae. Schweizerbart Verlag, 191–246.

Neustupa, J., & Němcová, Y. (2018). Morphological allometry constrains symmetric shape variation, but not asymmetry, of *Halimeda tuna* (Bryopsidales, Ulvophyceae) segments. PLoS One, 13(10), e0206492. doi:10.1371/journal.pone.0206492

Padisák, J., Soróczki-Pintér, É., & Rezner, Z. (2003). Sinking properties of some phytoplankton shapes and the relation of form resistance to morphological diversity of plankton – an experimental study. Hydrobiologia, 500(1–3), 243–257. doi:10.1023/a:1024613001147

Peña-Castro, J. M., Martínez-Jerónimo, F., Esparza-García, F., & Cañizares-Villanueva, R. O. (2004). Phenotypic plasticity in *Scenedesmus incrassatulus* (Chlorophyceae) in response to heavy metals stress. Chemosphere, 57(11), 1629–1636. doi:10.1016/j.chemosphere.2004.06.041

Phipson, B., & Smyth, G. K. (2010). Permutation p-values should never be zero: Calculating exact p-values when permutations are randomly drawn. Statistical Applications in Genetics and Molecular Biology, 9(1). doi:10.2202/1544-6115.1585

Piersma, T., & Drent, J. (2003). Phenotypic flexibility and the evolution of organismal design. Trends in Ecology & Evolution, 18(5), 228–233. doi:10.1016/s0169-5347(03)00036-3

Pozzobon, V., Levasseur, W., Guerin, C., Gaveau-Vaillant, N., Pointcheval, M., & Perré, P. (2020). *Desmodesmus* sp. pigment and FAME profiles under different illuminations and nitrogen status. Bioresource Technology Reports, 100409. doi:10.1016/j.biteb.2020.100409

R Core Team. (2024). R: A language and environment for statistical computing. https://www.R-project.org/

Riessen, H. P., & Gilbert, J. J. (2018). Divergent developmental patterns of induced morphological defenses in rotifers and *Daphnia*: Ecological and evolutionary context. Limnology and Oceanography. doi:10.1002/lno.11058

Rohlf, F. J. (1993). Relative-warp analysis and an example of its application to mosquito wings. Contributions to Morphometrics, 8, 131–159.

Rohlf, F. J. (2015). TPS Series. SB Morphometrics. http://www.sbmorphometrics.org/

Rohlf, F. J., & Marcus, L. F. (1993). A revolution in morphometrics. Trends in Ecology & Evolution, 8(4), 129–132. doi:10.1016/0169-5347(93)90024-j

Savriama, Y., & Klingenberg, C. (2011). Beyond bilateral symmetry: geometric morphometric methods for any type of symmetry. BMC Evolutionary Biology, 11(1), 280. doi:10.1186/1471-2148-11-280

Savriama, Y., Neustupa, J., & Klingenberg, C. (2010). Geometric morphometrics of symmetry and allometry in *Micrasterias rotata* (Zygnemophyceae, Viridiplantae). Nova Hedwigia, Beiheft, 136, 43–54. doi:10.1127/1438-9134/2010/0136-0043

Scheiner, S., & Levis, N. (2021). The loss of phenotypic plasticity via natural selection: Genetic assimilation. doi:10.1201/9780429343001-9

Shubert, E., Wilk-Wozniak, E., & Ligęza, S. (2014). An autecological investigation of *Desmodesmus*: implications for ecology and taxonomy. Plant Ecology and Evolution, 147, 202–212.

Stein, J. (1973.) Handbook of phycological methods: Culture methods and growth measurements. Cambridge University Press, 448.

Suzuki, Y., McKenna, K. Z., & Nijhout, H. F. (2020). Regulation of phenotypic plasticity from the perspective of evolutionary developmental biology. Phenotypic Switching, 403–442. doi:10.1016/b978-0-12-817996-3.00012-8

Trainor, F. R. (1992). Cyclomorphosis in *Scenedesmus communis* Hegew. Ecomorph expression at low temperature. British Phycological Journal, 27(1), 75–81. doi:10.1080/00071619200650091
Trainor, F. R. (1998). Biological aspects of *Scenedesmus* (Chlorophyceae) - phenotypic plasticity. Nova Hedwigia, Beiheft.

Trainor, F. R., Cain, J. R., & Shubert, L. E. (1976). Morphology and nutrition of the colonial green alga *Scenedesmus*: 80 years later. Botanical Review, 42(1), 5–25. http://www.jstor.org/stable/4353892

Téllez, T. R., & Møller, A. P. (2006). Fluctuating asymmetry of leaves in *Digitalis thapsi* under field and common garden conditions. International Journal of Plant Sciences, 167(2), 321–329. doi:10.1086/499613

Waddington, C. H. (1961). Genetic assimilation. Advances in Genetics, 257–293. doi:10.1016/s0065-2660(08)60119-4

Webster, M., & Sheets, H. D. (2010). A Practical introduction to landmark-based geometric morphometrics. The Paleontological Society Papers, 16, 163–188. doi:10.1017/s1089332600001868

West-Eberhard, M. J. (2008). Phenotypic plasticity. Encyclopedia of Ecology, 2701–2707. doi:10.1016/b978-008045405-4.00837-5

Woodard, K. (2023). Quantitative shape analysis of diatom frustules: asymmetry, allometry and morphospace structure (Dissertation). Charles University, Faculty of Science, Department of Botany, Prague. Supervisor: Jiří Neustupa.

Woodard, K., Kulichová, J., Poláčková, T., & Neustupa, J. (2016). Morphometric allometry of representatives of three naviculoid genera throughout their life cycle. Diatom Research, 31(3), 231–242. doi:10.1080/0269249x.2016.1227375

Yang, C.-H., & Pospisilik, J. A. (2019). Polyphenism – A window into gene-environment interactions and phenotypic plasticity. Frontiers in Genetics, 10. doi:10.3389/fgene.2019.00132

Yang, J., Li, B., Zhang, C., Luo, H., & Yang, Z. (2016). pH-associated changes in induced colony formation and growth of *Scenedesmus obliquus*. Fundamental and Applied Limnology / Archiv für Hydrobiologie, 187(3), 241–246. doi:10.1127/fal/2016/0846